Division of Invasive Cardiology, Department of Cardiology, Medical Faculty,

Albert Szent-Györgyi Clinical Center,
University of Szeged

NEW ASPECTS IN THE PATHOPHYSIOLOGY OF SEVERE AORTIC VALVE STENOSIS

Ferenc Tamás Nagy MD

PhD Thesis

Tutors:

Forster Tamás MD, PhD and Attila Nemes MD, PhD

2012

PUBLICATIONS RELATED TO THE DISSERTATION

I. Diehl P*, **Nagy F***, Sossong V, Helbing T, Beyersdorf F, Olschewski M, Bode C, Moser M. Increased levels of circulating microparticles in patients with severe aortic valve stenosis. Thromb Haemost 2008; 99: 711-9. Impact factor: 3.803

II. **Nagy FT**, Sasi V, Ungi T, Zimmermann Z, Ungi I, Kalapos A, Forster T, Nemes A. Correlations between myocardium selective videodensitometric perfusion parameters and corrected TIMI frame count in patients with normal epicardial coronary arteries. Int J Cardiol 2012; 155: 498-501. Impact factor: 6.802

III. **Nagy FT**, Horvath T, Ungi T, Sasi V, Zimmermann Zs, Kalapos A, Forster T, Ungi I, Nemes A. Aortic valve stenosis is associated with reduction in myocardial perfusion as assessed by videodensitometry on coronary angiograms. [Az aortabillentyű szűkülete együtt jár a koronarográfiás felvételeken videodenzitometria során meghatározott miocardialis perfúzió csökkenésével]. Orv Hetil 2012; 153: 1256-1262. Journal without impact factor.

OTHER PUBLICATIONS

I. Timinszky G, Tirián L, **Nagy FT**, Tóth G, Perczel A, Kiss-László Z, Boros I, Clarke PR, Szabad J. The importin-beta P446L dominant-negative mutant protein loses RanGTP binding ability and blocks the formation of intact nuclear envelope. J Cell Sci 2002; 115: 1675-87. Impact factor: 6.954

II. Nemes A, Kalapos A, Sasi V, Ungi T, **Nagy FT**, Zimmermann Z, Forster T, Ungi I. Detection of perfusion abnormalities on coronary angiograms in hypertension by myocardium selective densitometric perfusion assessments. Int J Cardiol 2012; 157: 428-9. Impact factor: 6.802

*These authors contributed equally

TABLE OF CONTENTS

LIST OF ABBREVIATONS

ACC: American College of Cardiology

AHA: American Heart Association

AMI: acute myocardial infarction

AS: aortic stenosis

AVS: aortic valve stenosis

CFR: coronary flow reserve

cpm: count per milliliter

CRP: C-reactive protein

CX: left circumflex coronary artery

DSA: digital subtraction angiography

LV-EF: left ventricular ejection fraction

ELISA: enzyme-linked immunosorbent assay

EMP: endothelial cell microparticle

G_{max}: maximal density

HUVEC: human umbilical vein endothelial cells

MBG: myocardial blush grade

MP: microparticle

LAD: left anterior descending coronary artery

LAO: left anterior oblique

LMP: leukocyte microparticle

MFI: mean fluorescence intensity

PBS: phosphate buffered saline

PC: patient control

PMP: platelet microparticle

PPP: platelet poor plasma

RC: right coronary artery

ROI: region of interest

TDC: time-density curve

TFC: thrombolysis in myocardial infarction frame count

TIMI: thrombolysis in myocardial infarction

T_{max}: time to reach maximal density

TMPG: thrombolysis in myocardial infarction myocardial perfusion grading

TNF-α: tumor necrosis factor alpha

Vmax: maximum velocity

1. INTRODUCTION

1.1. Aortic valve stenosis

1.1.1 Definition and epidemiology

Aortic stenosis (AS), characterized by obstruction of the left ventricular outflow tract is the most common valvular disease and the third most prevalent form of cardiovascular disease in the western world after hypertension and coronary artery disease. Present in 2% to 7% of patients older than 65 years, it is largely a disease of the elderly with prevalence increasing with age (1-2). The obstruction to the left ventricular outflow tract is localized most commonly at the aortic valve, a tricuspid semilunar valve regulating one-way blood flow between the left ventricle and the aorta. Obstruction less frequently may also occur above the valve (supravalvular stenosis) or below the valve (subvalvular stenosis), or maybe caused by hypertrophic cardiomyopathy, however these forms are not included in the scope of the current dissertation.

1.1.2 Pathophysiology and clinical presentation

Aortic valve stenosis (AVS) has three principal causes: rheumatic disease, congenital bicuspid valve and most commonly age-related calcification of the normal trileaflet valve which is further discussed in this thesis. Once considered to be caused by years of normal mechanical stress, the evolving concept is that the disease process represents proliferative and inflammatory changes similar but not identical to vascular calcification. Although association of AVS and systemic inflammation has been suggested in several studies and mononuclear cell infiltrations in the diseased valve ultimately leading to bone formation have been demonstrated, it remains unclear how inflammation is triggered and maintained (3-6). Cardinal manifestations of AVS are exertional dyspnea, angina, syncope and ultimately heart failure usually presenting only in severe cases (7). Physiological alterations behind angina pectoris-like symptoms are dominantly supplied by left ventricular mass increment leading to increased oxygen consumption, decreased arteriole density, coronary diastolic filling impediment and subsequently subendocardial ischemia (8, 9). In about 50% of the cases associated significant coronary artery obstruction may further worsen symptoms (7). Beside the model dominated by left ventricular pathologic alterations, generalized endothel dysfunction described not only in severe aortic valve stenosis but already in aortic valve

sclerosis (10-11) may also play a role in development of angina pectoris by affecting the coronary arteries.

1.1.3 Treatment modalities

To date there is no clinically proven medical therapy to affect disease progression. Based on common risk factors and similar pathology with vascular atherosclerosis several lipid lowering trials with intensive statin therapy have been completed. These studies convincingly showed no improvement in rate of progression, mortality or time to aortic valve replacement compared to placebo (12-13), shifting interest to other pathological pathways possibly amenable to medical therapy. Surgical aortic valve replacement or transcatheter aortic valve replacement in case of patients seriously ill and not candidates for conventional surgery remains the treatment of choice for patients with severe AVS. Indication and timing of surgery is based upon patient symptoms, echocardiographic findings and confounding diseases as aortic aneurysm, coronary artery disease also necessitating thoracic surgery (14).

1.2. Cell derived microparticles

1.2.1 Definition

Microparticles (MPs) are small cell membrane vesicles that are shed from cells upon activation. MPs can be detected and classified by their particular set of surface antigens. Using these means, platelet, leukocyte and endothelial microparticles can be distinguished and attributed to their respective cell of origin (15).

1.2.1 Role in cardiovascular diseases

MPs exert distinct physiological functions and transfer biological information between different cell types by carrying a specific set of signaling molecules between the cell of origin and the effector cells (16). Particularly, in the vascular compartment MPs are essential for intercellular crosstalk in health and disease (17). Although the pathophysiologic mechanisms and functions of MPs are not completely understood, it is clear that chronic vascular diseases such as peripheral artery disease or diabetic vascular disease are associated with elevated levels of circulating MPs. Furthermore, MPs are also associated with systemic cell activation such as systemic inflammation, sepsis or rheumatic diseases (18, 19). By the presentation of

cell-cell interacting surface molecules such as P-selectin and coagulation factors MPs may contribute to endothelial cell activation, leading to vascular inflammation and frequently to the development of atherosclerosis, but also to angiogenesis (15, 20-23). Taken together, MPs are important players in the pathophysiology of vascular diseases and may also be used as in-vivo markers for inflammation and vascular damage.

1.3. Angiography-derived modalities for the assessment of myocardial perfusion in the catheterization laboratory

1.3.1 Thrombolysis in myocardial infarction (TIMI) frame count

A quantitative variation of the TIMI flow grade, TIMI frame count (TFC), defined as the number of frames required for contrast material to travel from the coronary ostium to a distal landmark was introduced in the 1990s as a method to assess the efficacy of thrombolysis in acute myocardial infarction (AMI) on coronary angiograms (24). TFC proved to be a simple, reproducible, quantitative and objective method to evaluate epicardial flow not only in acute coronary syndrome settings, but in other conditions with microvascular dysfunction, as well (25). For instance, abnormal TFCs have been found to support evidence of microvascular dysfunction, increased microvascular resistance in metabolic X syndrome, aortic valve stenosis, hypertrophic cardiomyopathy, cardiac allograft vasculopathy and atrial fibrillation (26-30). However, both TIMI flow score and TFC remain indirect measures of microvascular flow and patency. Tissue level perfusion is not assessed by these parameters, which is the final goal of reperfusion therapy

1.3.2. Myocardial blush grade and TIMI myocardial perfusion grade

Two different angiographic methods were described in the late 1990s for direct assessment of myocardial perfusion on a coronary angiogram based on the angiographic “blush” phenomenon. When contrast medium is properly injected and cine acquisition is sufficiently prolonged, the filling of myocardial vasculature appears as an angiographic “blush,” or a “ground-glass” appearance. This appearance can be used in the catheter laboratory to visually assess microvascular filling and, hence, is a marker of microvascular dysfunction and no-reflow (31). While, myocardial blush grade (MBG) measures the maximal intensity of contrast opacity at the area at risk (32), TIMI myocardial perfusion grading (TMP) classifies reperfusion based on the dynamics of contrast appearance and clearance (33). These methods

have provided additional prognostic information on success of reperfusion therapy in AMI compared to TFC (33). However they remain limited inherently by their subjective nature and categorical values.

1.3.3. Computer assisted, myocardium selective videodensitometry

Recently novel computer-assisted videodensitometric methods have been introduced for the quantitative assessment of the angiographic "blush" appearance (34-36) in AMI. Alongside Korosoglou *et al*. we have characterized myocardial perfusion by the ratio of maximal density (G_{max}) and the time to reach maximum density (T_{max}) of the time–density curves (TDCs) in regions of interest on X-ray coronary angiograms (37). Sensitized by vessel masking technique, it supplies easily obtainable, objective and quantitative information on short-term outcome in AMI (37, 38). However, potential use of these methods for evaluating myocardial perfusion, microvascular dysfunction in the non acute coronary syndrome patient population is not well documented.

2. AIMS

1. To determine the level of microparticle release and systemic inflammation in patients with severe aortic valve stenosis and thereby to elucidate the role of microparticles in the origin and progression of the disease.

2. To establish the relation between our novel computer-assisted, myocardium selective videodensitometric method for regional myocardial perfusion assessment and the TIMI frame count method in patients with epicardial coronary arteries without significant stenosis.

3. To demonstrate myocardial perfusion abnormalities in patients with severe aortic valve stenosis without significant epicardial coronary artery stenosis by computer-assisted, myocardium selective videodensitometric measurement.

3. PATIENTS AND METHODS

3.1. Cell derived microparticles in aortic valve stenosis

3.1.1. Patients

From May 2005 to November 2006, 22 patients with AVS were enrolled prospectively in our first study at the Department for Cardiology and Angiology, University Hospital Freiburg. As control we examined 18 individuals that were admitted to our department for chest pain of unknown origin and in which an acute coronary syndrome, vascular disease and other relevant medical conditions were excluded. All participants were instructed about the aims of the study and gave their written informed consent. The study was approved by the local Ethics Committee. We excluded patients and patient controls with diseases in which an increased level of MPs is known, such as acute myocardial infarction, metabolic syndrome, insulin dependent diabetes mellitus, peripheral artery disease, severe trauma, sepsis, encephalitis disseminata, as well as patients with systemic diseases such as chronic infection, renal failure and history of cancer (22, 39-47) (Table 1). Standard blood analysis (blood cell count, plasma coagulation parameters, cardiac enzymes, C-reactive protein (CRP), retention parameters and lipid profile) was performed in each participant.

Table 1. Inclusion and exclusion criteria for the recruitment of AVS patients. To recruit patient controls the same criteria except for aortic valve surface were applied.

Inclusion criteria	**Exclusion criteria**
Written informed consent	Acute coronary syndrome
Age > 18 years	Peripheral artery disease
Aortic valve surface area <1cm²	Insulin dependent diabetes mellitus
	Metabolic syndrome
	Infectious disease/ sepsis/fever/ leukocytosis (>10 x 10^3/µl), C-reactive protein > 10 mg/l
	Systemic inflammatory disease
	Rheumatic disease
	Renal failure

3.1.2. Echocardiography

AVS was defined as an aortic valve surface of 1.0 cm² or less, according to the American College of Cardiology (ACC)/ American Heart Association (AHA) guidelines for valvular heart disease (14). All AVS patients had chronic degenerative AVS. Patients with congenital valve disease or a history for rheumatic AVS were excluded. To exactly quantify the extent of AVS, all AVS patients underwent transthoracic echocardiography using a PHILIPS iE33© (Netherlands) ultrasound system and a 3.5 MHz transducer. Images were acquired in accordance with the guidelines of the American Society of Echocardiography (48).

3.1.3. Flow cytometry

CD31-PE and CD61-FITC antibodies were obtained from Dako. CD45-FITC, CD62P-PE, CD62E-PE, CD11b-PE antibodies were obtained from Becton Dickinson. CD11b-FITC was from Beckman Coulter. All antibodies were diluted 1:10 and passed through a 0.22-µm filter before use. Venous blood was collected without application of a tourniquet into 5 ml containers to a final concentration of 0.1 mM citrate using a 21-gauge butterfly needle (WING-FLOTM, Mainz, Germany). Analysis was initiated within 1 hour (49). Samples were centrifuged at 1,550 g for 20 minutes (min) at 20°C to obtain platelet-poor plasma (PPP). PPP aliquots were incubated with the specific antibodies for 25 min in the dark before sterile filtered phosphate buffered saline (PBS) was added up to a total volume of 500 µm and microparticles were quantified by flow cytometry (FACS-Calibur©, Becton Dickinson) and CellQuestTM software (Version 3.3, Becton Dickinson). Size calibration was performed with nonfluorescent polystyrene microspheres (Invitrogen Molecular Probes©, USA). Each sample tube was measured with a flow rate of 35 µl/min for 60 seconds. MPs were distinguished from blood cells by their size of <1.5 µm and numbers are given in counts per min (cpm) (Fig. 1A). Platelet microparticles (PMPs) were detected as CD31+/CD61+ particles <1.5 µm of size or as CD62P+/CD61+ particles <1.5 µm, termed CD62P+ throughout this article (Fig. 1B, 1C). Leukocyte microparticles (LMPs) were defined as CD11b+ particles smaller than 1.5 µm (50). Endothelial cell microparticles (EMPs) were defined as CD62E+ particles smaller than 1.5 µm originating from endothelial cell activation (Fig. 1F, 1G) (51). To quantify monocyte activation, whole blood (100 µl) was incubated gently shaking in the dark with 10 µl anti-CD11b-PE. After suspension in 2 ml cell lyses solution (tris-base, Na2EDTA, SDS), samples were incubated for 20 min to lyse erythrocytes before centrifugation with 500 g for 5 min.

The supernatant was removed and after washing twice with 2 ml PBS (Mg2+Ca2+) analyzed by flow cytometry. Monocytes were defined as CD11b+ cells within the appropriate monocyte gate (40, 52 and 53). For quantification of granulocyte activation, CD11b+ cells were gated to include the granulocyte population. Activated leukocytes were quantified in fluorescence histograms, and medians were used for further statistical analysis as mean fluorescence intensity (MFI). Monocyte-PMP conjugates were assessed by detection of particles that were positive for both CD45 and for CD62P after gating the monocyte population in forward/sideward scatter. To detect conjugates between activated monocytes and PMPs CD11b antibody was used instead of CD45 antibody and samples were processed as described above. PMP-monocyte conjugates may not be distinguishable from platelet-monocyte conjugates.

3.1.4. Flow chamber experiments

To mimic different levels of shear stress *in vitro* we used the Glycotech flow chamber with gasket C. Flow was induced using a Harvard apparatus syringe pump (phd 2000). Flow rates were adjusted as described to achieve shear forces of 0.5 dynes/cm^2 and 15 dynes/cm^2. Citrated whole blood was obtained and subjected to the respective shear forces prior to analysis of MPs using our standard protocol.

3.1.5. Plasma levels of soluble P-selectin and interleukin-6 (IL-6)

Blood concentrations of soluble P-selectin and IL-6 were determined from patient plasma that was obtained by centrifugation of citrated blood directly after collection and that was stored until assaying at –80°C. Commercial enzyme-linked immunosorbent assay (ELISA) kits were obtained and used as recommended by the manufacturer (R&D Systems, Dako).

3.1.6. Statistical analysis

Data are presented as absolute and relative frequencies for categorical variables and as means with standard deviations for continuous variables. Correlations between selected variables were estimated by Spearman's rank correlation coefficient. Data of AVS and control patients was compared by means of Fisher's exact test for categorical variables and by the Wilcoxon

rank test for continuous variables. All tests were two-sided and used a significance level of 5%. Data were analyzed with SAS version 9.1 (SAS Institute Inc., Cary, NC, USA).

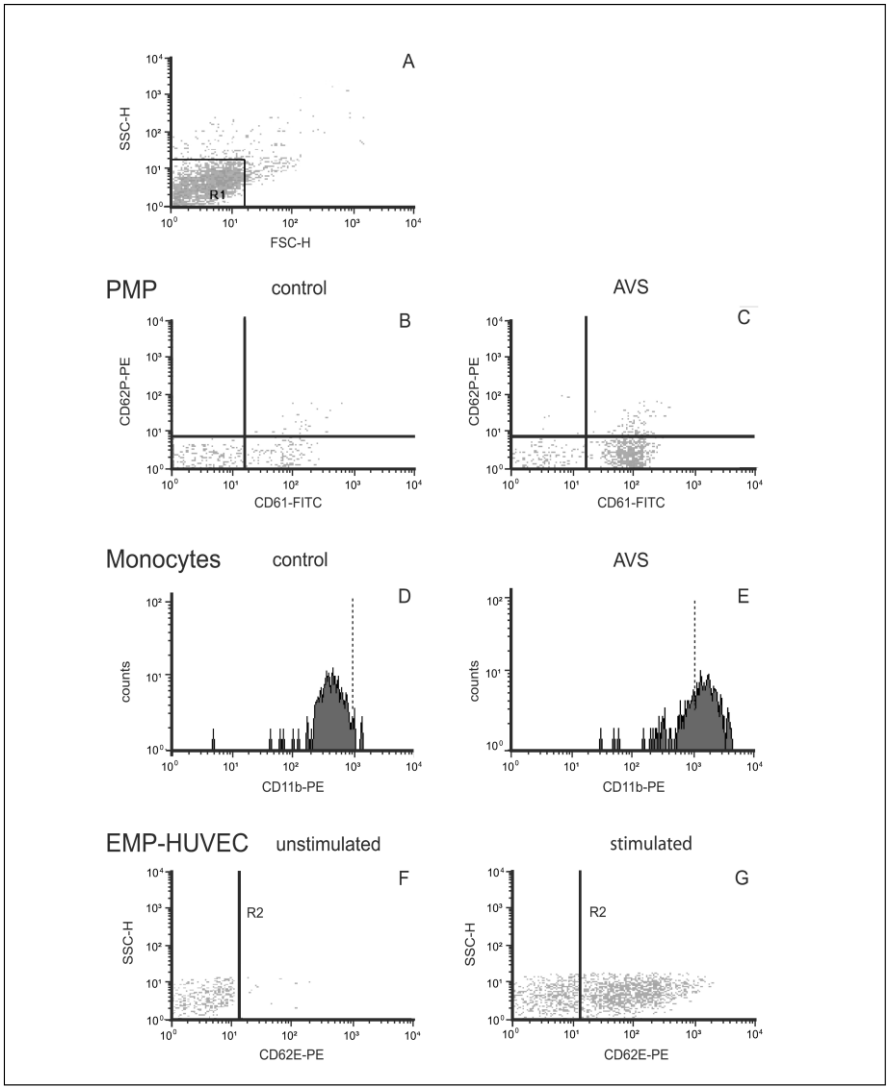

Figure 1. *Detection of microparticles. A) Gating strategy based on forward-sideward scatter. Platelet poor samples were scanned for size and granularity. Particles smaller than 1.5 µm, as determined by calibration beads, were included in region 1 (R1) for further analysis. B and C) Example for PMP classification based on CD61 and CD62P in a control individual compared to an AVS patient. The upper right quadrant contains CD61+/CD62P+ MPs, the lower right quadrant contains CD61+/CD62- MPs. These MPs have been shown to be also CD31 positive in parallel aliquots. D and E) Example for detection of activated monocytes. In control individuals fluorescence is lower compared to AVS patients as demonstrated in relation to the dotted line at* 10^3*. F and G) In vitro positive control for EMP measurement. HUVEC were stimulated by TNF-α and CD62E+ MPs were detected in the supernatant.*

3.2. Evaluation of the relationship between computer-assisted myocardium selective videodensitometry and TIMI frame count

3.2.1 Patients

The second study comprised 43 patients with chest pain who had undergone elective coronary angiography with a negative result (<40% intraluminal epicardial coronary artery diameter stenosis) at the Division of Invasive Cardiology, Department of Cardiology, Medical Faculty, Albert Szent-Györgyi Clinical Center, University of Szeged. Patients with acute coronary syndrome, valvular heart disease and left ventricular dysfunction were excluded from this study. Informed consent was obtained from each patient and the study protocol conformed to the ethical guidelines of the 1975 Declaration of Helsinki.

3.2.2. Technical aspects of coronary angiography

Angiograms for videodensitometric analysis were recorded as described by our working group previously (37). Briefly this required the fulfillment following criteria: 1) motion of patient or table should be avoided, 2) patient should hold breath for the time of recording, 3) one contrast-free heart cycle should be recorded before injection of contrast material, and 4) field of view is to be set to contain the whole supplied area of the vessel of interest. During the present study, all coronary angiograms met with these criteria. Patients not being able to hold breath for the time of recording were excluded from this study. Projections were chosen to minimize the possible superpositioning of the myocardium supplied by different arteries, aorta, veins and the edge of the diaphragm which usually gives motion artifacts on digital subtraction angiography (DSA) images. Left anterior descending coronary artery (LAD) and left circumflex coronary artery (CX) were recorded in lateral, while right coronary artery (RC) was recorded in a left anterior oblique (LAO 15') projection. Constant quantity of nonionic contrast material (6ml) was injected for all angiograms by an automatic injector (Acist Medical Systems, Bracco, Milan, Italy) at a rate of 3 cc/sec in order to standardize the density of angiograms. Coronary angiograms were recorded on an Innova 2000™ system (GE Healthcare, Chalfont St. Giles, Buckinghamshire, United Kingdom), images were stored in 512×512 size 8-bit, grayscale, uncompressed format.

3.2.3. Videodensitometric analysis

Videodensitometric analysis was performed as reported by our working group previously (37). Briefly phase-matched DSA angiograms were recorded with constant contrast, brightness and stabilized acquisition parameters of the X-ray imaging system. The computerized method for myocardial perfusion assessment was based on the analysis of time-density curves (TDCs) measured over the myocardial region of interest (ROI). Polygonal shaped ROIs were selected by an experienced interventional cardiologist and covered the whole myocardial area supplied by the investigated vessel. Specific coronary-related ROIs are presented in Figure 2. TDCs were calculated as average pixel value in the ROI, excluding pixels having a vesselness probability value >0.08. Frequencies higher than 0.6 Hz have been removed from the TDC to eliminate artifacts from cyclic heart contractions, and noise in image acquisition and digital subtraction. Myocardial perfusion has a single-wave density signal around 0.1 Hz; therefore it is still present on the filtered curve. A typical TDC before and after filter application is shown in Figure 3. Maximal density of the TDC (G_{max}) and time to reach maximal density (T_{max}) were measured on the filtered curve. Perfusion was characterized by Gmax/Tmax according to previous results (34). Vessel masking technique was used to further improve sensitivity (38). To get more reliable results two independent physicians were required to select the myocardial area supplied by the coronary vessel, and draw a polygonal ROI. Two G_{max}/T_{max} values calculated with the two different ROIs were averaged, and these results were used to analyze correlation with other clinical parameters. Cardiologists were blinded to all other clinical data.

3.2.4. Assessment of TIMI frame count

Determination of frame counts was carried out by the method described previously by Gibson *et al.* (Figure 4.) (24).The first frame was defined by a column of contrast extending across > 70% of the arterial lumen with ante grade motion. The last frame counted is that in which contrast enters (but not necessarily fills) a distal landmark. These landmarks are as follows: the first branch of the posterolateral artery in the RC, the distal branch of the lateral left ventricular wall artery furthest from the coronary ostium in CX, and the distal bifurcation known as the “moustache,” “pitch fork,” or “whale's tail” in LAD. LAD-TFC was corrected by a factor (1.7) to take account for longer distance to the TIMI landmark to gain corrected TIMI frame count (cTFC) (24). In addition, a conversion factor of 2 was used to adjust for frame rate of 15 frame/sec used in our laboratory compared to the 30 frame/sec acquisition speed used in the original cine angiographic studies (55).

3.2.5. Statistical analysis

Data are reported as means ± standard deviation. Data analyses were performed with statistical software Medcalc (Medcalc 11.3, Mariakerke, Belgium). P <0.05 was considered to be statistically significant. Correlations of G_{max}/T_{max} with cTFC were assessed by Spearman's rank correlation coefficient. Values for R were interpreted in the following way: 0.9-1: excellent, 0.7-0.89: good, 0.5-0.69: moderate, 0.3-0.49: low.

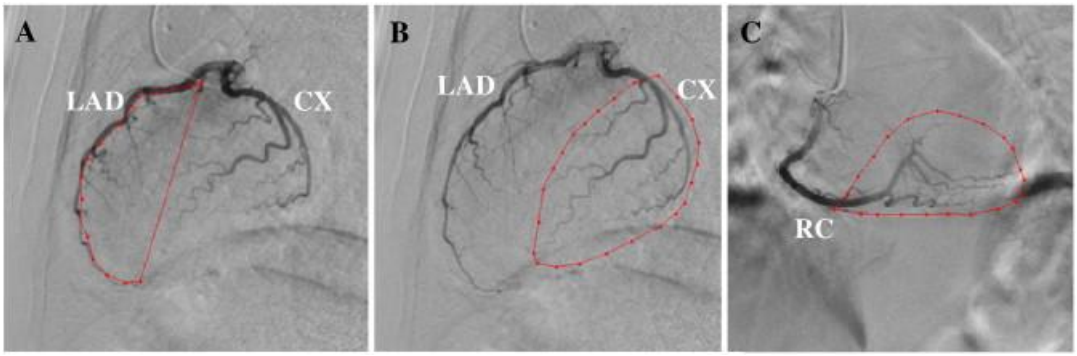

Figure 2. *Coronary artery related territories on coronary angiograms. LAD (A), CX (B) and RC (C).*

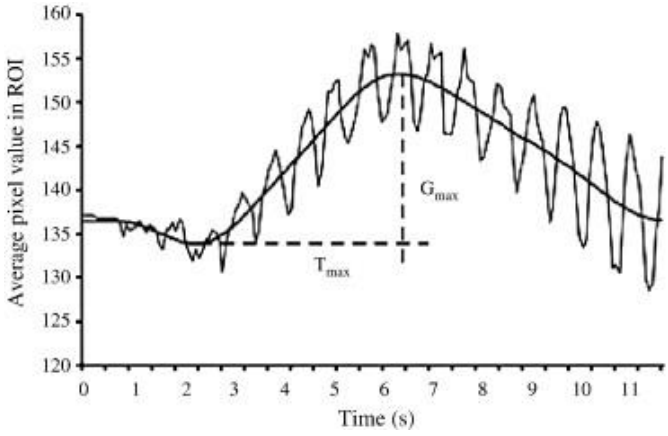

Figure 3*. Schematic diagram of videodensitometric measurement result. Thinner curve represents the original average density. The thicker curve is computed by eliminating frequencies higher than 0.6 Hz from the original curve. Myocardial perfusion is characterized by the ratio of maximal density (G_{max}) and the time to reach maximum density (T_{max}).*

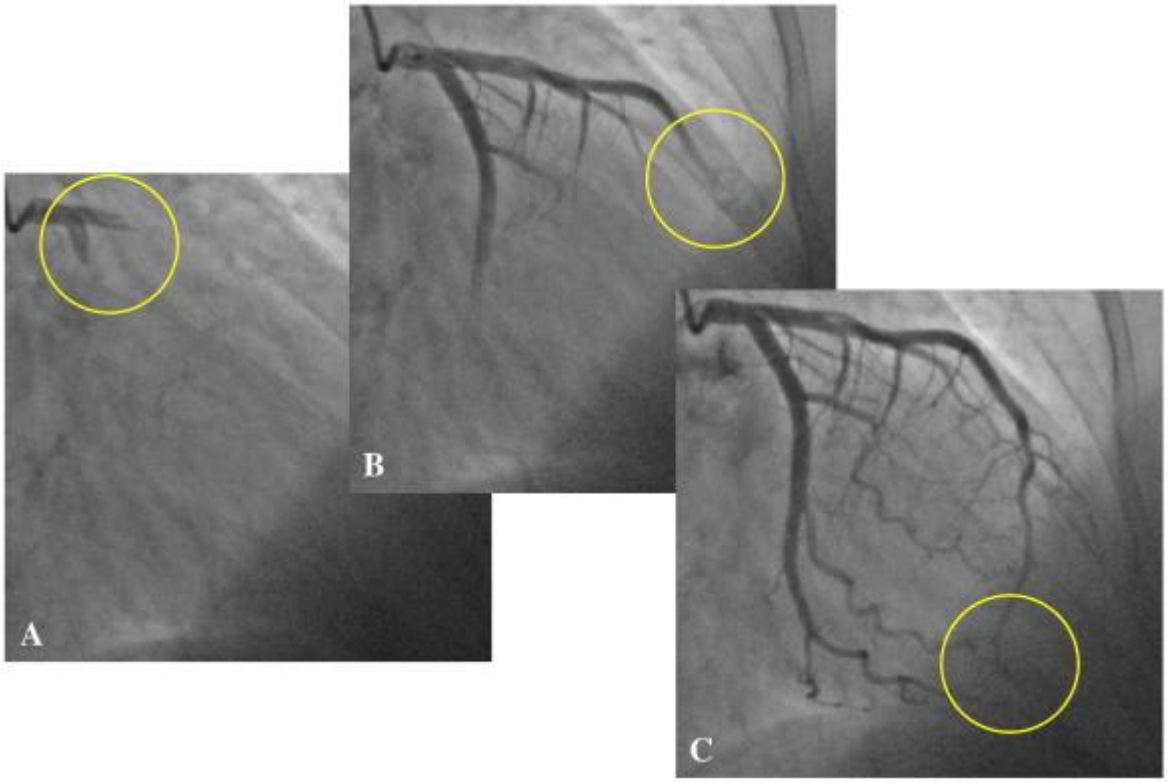

Figure 4. *Angiographic image of the left anterior descending coronary artery (LAD) for measurement of TIMI frame count. The first frame (A) defined by a column of contrast extending across >70% of the arterial lumen with antegrade motion. Intermediate (B) and last (C) frames with contrast reaching the distal landmark of LAD.*

3.3. Myocardial perfusion abnormalities in aortic valve stenosis as assessed by computer-assisted, myocardium selective videodensitometry

3.3.1. Patients

The third study comprised 20 patients with aortic valve stenosis who were omitted to Division of Invasive Cardiology, Department of Cardiology, Medical Faculty, Albert Szent-Györgyi Clinical Center, University of Szeged for cardiac catheterization as a part of the preoperative examination protocol before aortic valve replacement surgery. Patients with significant coronary artery disease (>70% intraluminal epicardial coronary artery diameter stenosis) were excluded from the study. 30 patients omitted for evaluation of chest pain of unknown origin but diagnosed to be without significant coronary artery disease served as a control group. The control group was matched in regards to age, gender and ischemic heart disease risk factors.

Informed consent was obtained from each patient and the study protocol conformed to the ethical guidelines of the 1975 Declaration of Helsinki.

3.3.2. Technical aspects of coronary angiography

The same technical features were used for coronary angiography as described in section 2.2.2.

3.3.3. Videodensitometric analysis

The same technical features were used for videodensitometric analysis as described in section 2.2.3. In addition to single vessel related G_{max}/T_{max} values we introduced mean G_{max}/T_{max} (average of single vessel related G_{max}/T_{max} values) to describe global myocardial perfusion. Representative DSA angiograms and TDCs for AVS and control patients are shown in Figure 5.

3.3.4. Statistical analysis

Data are presented as absolute and relative frequencies for categorical variables and as means with standard deviations for continuous variables. Data of AVS and control patients were compared by means of Pearson's chi square test for categorical variables and by the Student's T test for continuous variables. In case of the LAD related G_{max}/T_{max} Welch's test was used because of unequal variance. All tests were two-sided. $P < 0.05$ was considered to be statistically significant. Statistical software applied was Medcalc (Medcalc 11.3, Mariakerke, Belgium).

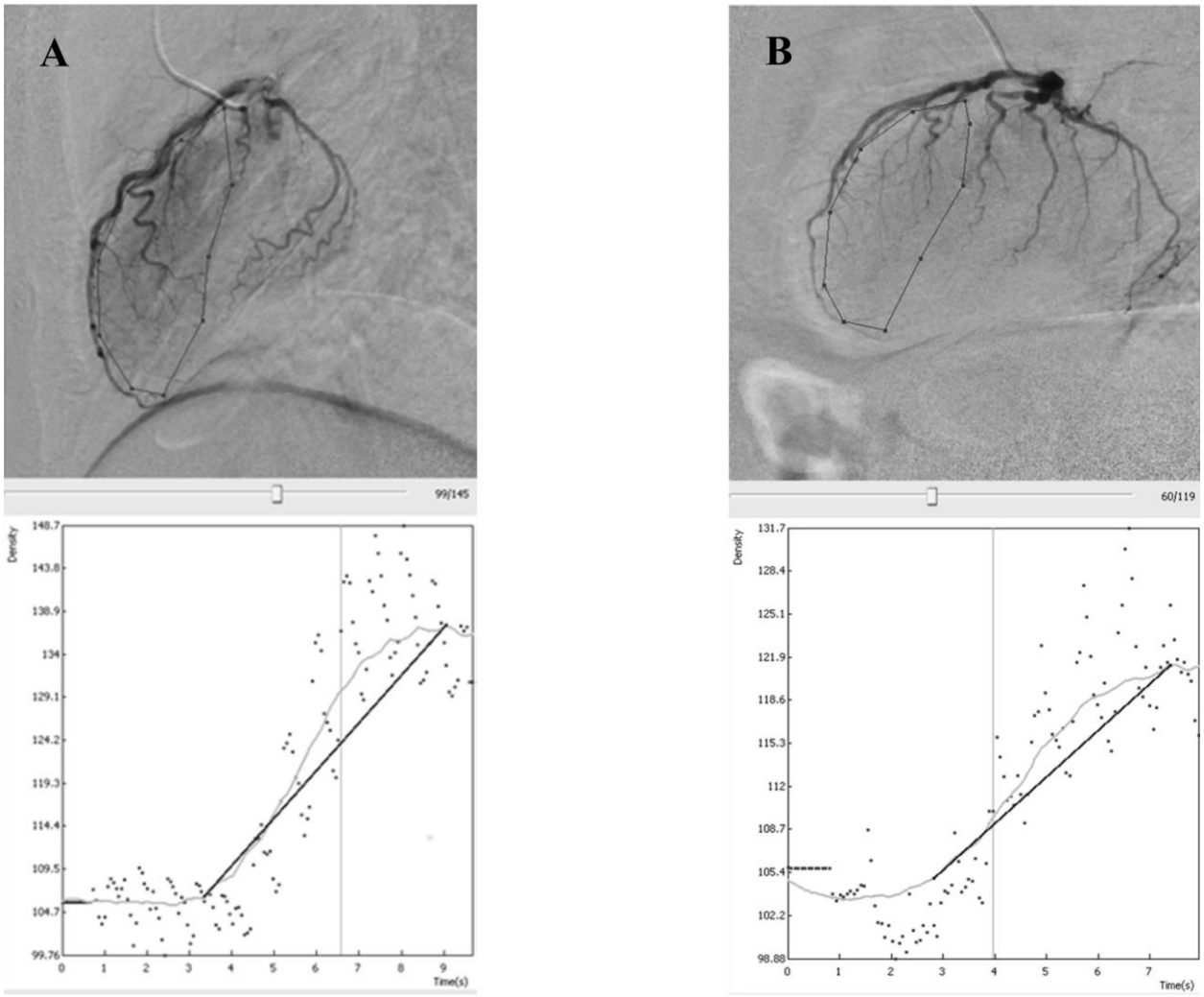

Figure 5. *DSA angiogram and corresponding TDC curve. Upper panels show a frame of the DSA angiogram of the left coronary artery with black line surrounding the region of videodensitometric measurement concerning the LAD. Lower panels show the corresponding time-density curves and videodensitometric measurement results. (A)Control, (B)AVS patient.*

4. RESULTS

4.1. Cell derived microparticles in aortic valve stenosis

4.1.1. Clinical parameters

As shown in Table 2, AVS patients and patient controls (PC) were similar in terms of age (AVS: 71.4 ± 11.8 vs. PC: 67.3 ± 9.3 years), gender distribution (female male ratio: AVS: 13:9 vs. PC: 9:9), cardiovascular risk factors, blood cell counts, CRP level, cholesterol and body mass index. Notably, there was no significant difference in antiplatelet medication.

Table 2. Clinical characteristics of aortic valve stenosis patients and patient controls.

	AVS patients	**Patient controls**
N	22	18
Age (years)	71	67
Gender		
Female	13	9
Male	9	9
Platelets (10^3/μl)	237	235
Leukocytes (10^3/μl)	6.63	7.09
C-reactive protein (mg/dl)	6.9	8.4
Cholesterol (mg/dl)	177	200
Antiplatelet medication (%)	32	28
Cardiovascular risk factors		
Smoking (%)	14	6
Hypercholesterolemia (%)	33	28
Hypertension (%)	73	78
Diabetes mellitus (%)	23	39
BMI (height/weight²)	25	27

4.1.2. Echocardiographic parameters

The mean of the aortic valve surface of AVS patients was 0.65 ± 0.16 cm², resulting in an elevated transvalvular gradient of 73 ± 28 mmHg and increased blood velocity (Vmax) (Table 3). Patient controls had no signs for morphologic heart disease. Average left ventricular ejection fraction (LV-EF) was similar with 53 ± 13% in AVS patients compared to 57 ± 4% in patient controls. Accordingly, left ventricular end diastolic diameter was similar in both groups. In order to estimate transvalvular shear stress we calculated the Vmax/LV-EF ratio. As expected for severe aortic stenosis Vmax/LV-EF was significantly increased in AVS patients compared to patient controls (Figure 6A).

Table 3. Echocardiographic characteristics of aortic valve stenosis patients and patient controls. NS =not significant.

	AVS patients	**Patient controls**	**p**
Aortic valve surface (cm²)	0.65 ± 0.16	>1.5	<0.05
Vmax (m/s)	4.1 ± 1	1.4 ± 0.4	<0.05
Mean transvalvular aortic gradient (mmHg)	73 ± 28	9± 5	<0.05
Left ventricular ejection fraction (LV-EF) (%)	53 ± 13	57 ± 4	NS
Left ventricular end diastolic diameter (mm)	49.8 ± 11.5	49.5 ± 4	NS
Vmax/LV-EF	0.08 ± 0.03	0.02 ± 0.01	<0.05

4.1.3. Platelet microparticles

The number of total PMPs (CD31+/CD61+) was significantly higher in AVS patients compared to patient controls (AVS: 868 ± 600 cpm vs. PC: 504 ± 230 cpm, p= 0.046, Fig. 6B). In patients with AVS CD62P+ PMPs were also significantly increased (AVS: 76.0 ± 44.5 cpm vs. PC: 47.8 ± 21.8 cpm, p= 0.028, Fig. 6C). No significant differences in platelet

counts between both groups were observed (AVS: 237 ± 70/nl vs. PC: 235 ± 69/nl, p = 0.92, Fig. 6B) indicating that differences in PMPs do not originate from differences in platelet counts. In order to demonstrate the relationship between shear stress and PMP activation, we correlated these two parameters in Figure 6D. PMP activation increased with augmenting shear stress in our patients. These data support the notion that platelet microparticles are increased in AVS patients most likely due to increased blood shear stress in these patients.

4.1.4. Flow chamber experiments

As we have demonstrated shear stress-induced PMP generation in AVS patients we sought to corroborate these data by in-vitro experiments. Therefore we subjected whole blood from volunteers (n=4) to various levels of shear stress in a flow chamber and analyzed the generation of PMPs. In these experiments increasing shear forces significantly induced increasing amounts of PMPs, indicating that shear stress is a trigger for PMP release (Figure 7).

4.1.5. Leukocyte microparticles (LMPs)

Patients with AVS had significantly more LMPs compared to patient controls (AVS: 31.6 ± 18.5 cpm vs. PC: 19.4 ± 9.7 cpm, p =0.014, Figure 8A). The number of leukocytes in the peripheral blood was similar in both groups (AVS: 6.63 ± 2.00 10^3/µl vs. PC: 7.09 ± 1.85 10^3/µl; p =0.34, Table 2). As shown above for PMPs, the generation of LMPs is independent from the numbers of the cells of origin. These data support the notion that the number of LMPs is elevated in AVS patients reflecting an inflammatory state in AVS patients.

4.1.6. Leukocyte activation

As the elevated numbers of LMPs indicate an inflammatory state in AVS patients we sought to quantify the extent of leukocyte activation. Therefore we measured CD11b+ monocytes and granulocytes. Activated monocytes were increased in AVS patients compared to patient controls (AVS: 902 ± 331 MFI vs. PC: 676 ± 189 MFI; p =0.042, Figure 8C). Accordingly, there was a trend towards increased numbers of activated granulocytes in AVS patients (AVS: 437 ± 216 MFI vs. PC: 339 ± 82 MFI; p =0.062, Fig. 8C). Thus, not only numbers of LMPs but also numbers of their activated cells of origin are increased in AVS patients.

4.1.7. Endothelial microparticles

To reflect endothelial cell activation we determined the number of circulating EMPs. The amount of CD62E+ EMPs was elevated in AVS patients compared to patient controls (AVS: 19.7 ± 12.3 cpm vs. PC: 10.4 ± 6.8 cpm, p =0.008, Figure 8B), indicating endothelial cell activation in AVS patients. Most interestingly the extent of monocyte activation correlates with the number of CD62E+ EMPs (Figure 8D) supporting the hypothesis that monocyte activation contributes to activation of endothelial cells in AVS patients. Conversely, we cannot rule out that EMPs contribute to monocyte activation in AVS patients.

4.1.8. PMP-monocyte conjugates

To elucidate the mechanism of monocyte activation we determined the number of circulating PMP-monocyte complexes in four representative patients with AVS and four controls. The number of total PMP-monocyte complexes was higher in AVS patients compared to controls (Figure 9A) Using an activation specific antibody (CD11b) we found that almost all PMP-monocyte complexes contained activated monocytes (Figure 9B). This may be due to the fact that PMPs have the potential to activate monocytes or inversely that activated monocytes have a higher affinity to PMPs. Therefore we suggest that binding of PMPs results in activation of monocytes.

4.1.9. Blood levels of soluble P-selectin and IL-6

Besides the number of circulating microparticles representing “cellular markers” for platelet activation, soluble P-selectin was measured in the blood of AVS patients and patient controls. We found that plasma P-selectin levels were not significantly different between AVS patients and patient controls with a trend to higher concentrations in AVS patients (Figure 10). To determine a plasmatic marker for systemic inflammation we measured plasma concentrations of IL-6. In AVS patients IL-6 tended to be higher than in patient controls without reaching statistical significance (Figure 10). These data indicate that P-selectin and IL-6 may not be as sensitive as microparticle counts to detect a systemic state of inflammation and platelet activation.

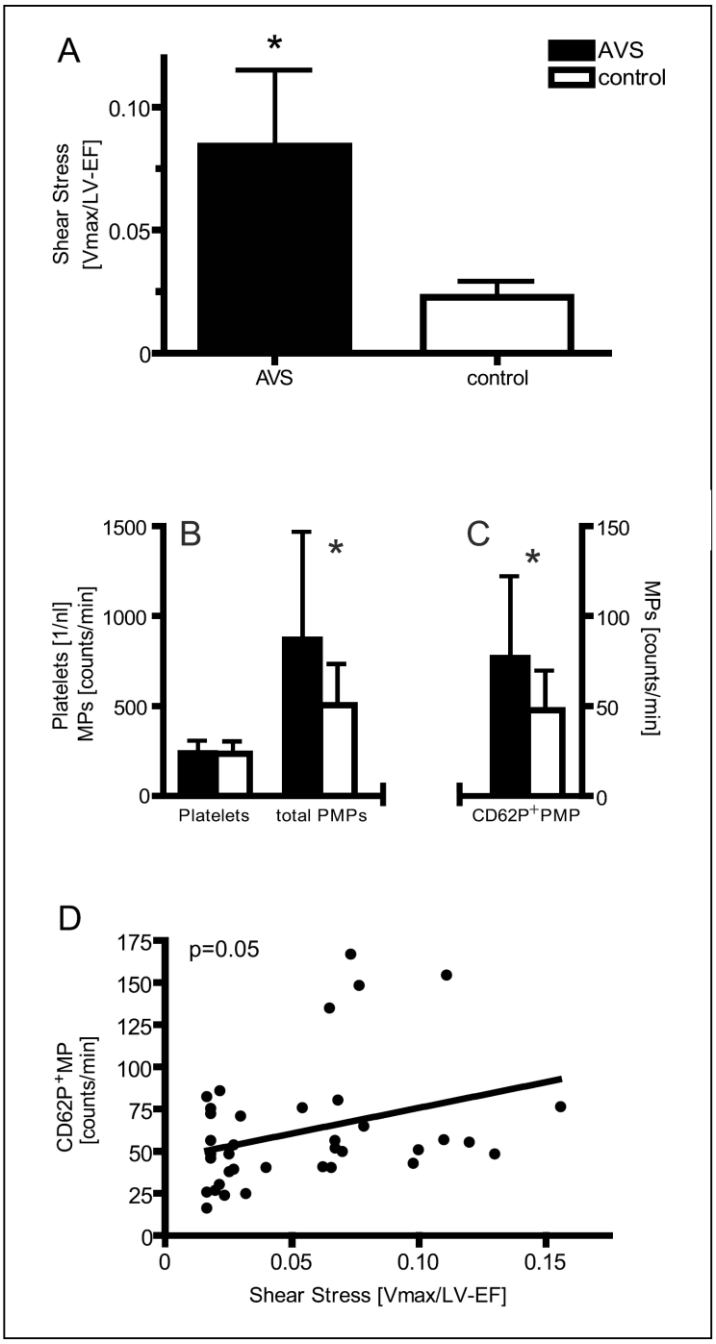

Figure 6. *Valvular shear stress and platelet microparticles. A) Vmax/LV-EF ratio representing the individual valvular shear stress is significantly increased in AVS patients. B) The number of circulating platelets is not different between the groups. Patients with AVS have more circulating PMPs. C) CD62P+PMPs, so called "activated PMPs", are also elevated in AVS patients. D) Correlation between valvular shear stress and CD62P+PMPs (correlation coefficient =0.32). * indicates p< 0.05, AVS versus control.*

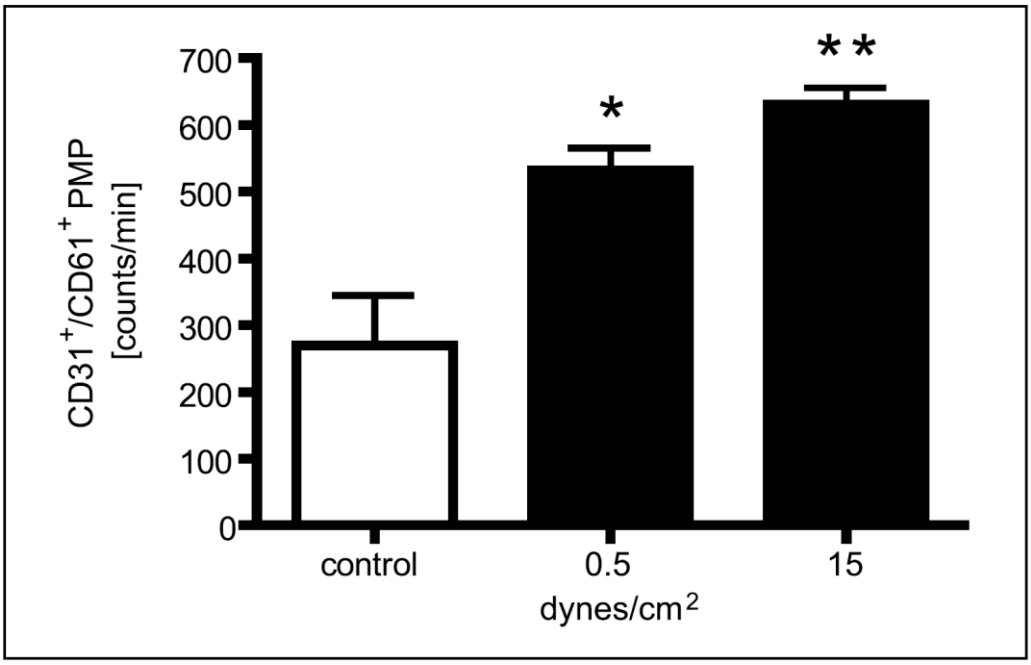

Figure 7. *Shear stress and PMP release in vitro. Increasing shear stress induced in vitro results in increasing numbers of CD31+/61+PMPs. * indicates p<0.05 versus control; ** indicates p <0.01 versus control.*

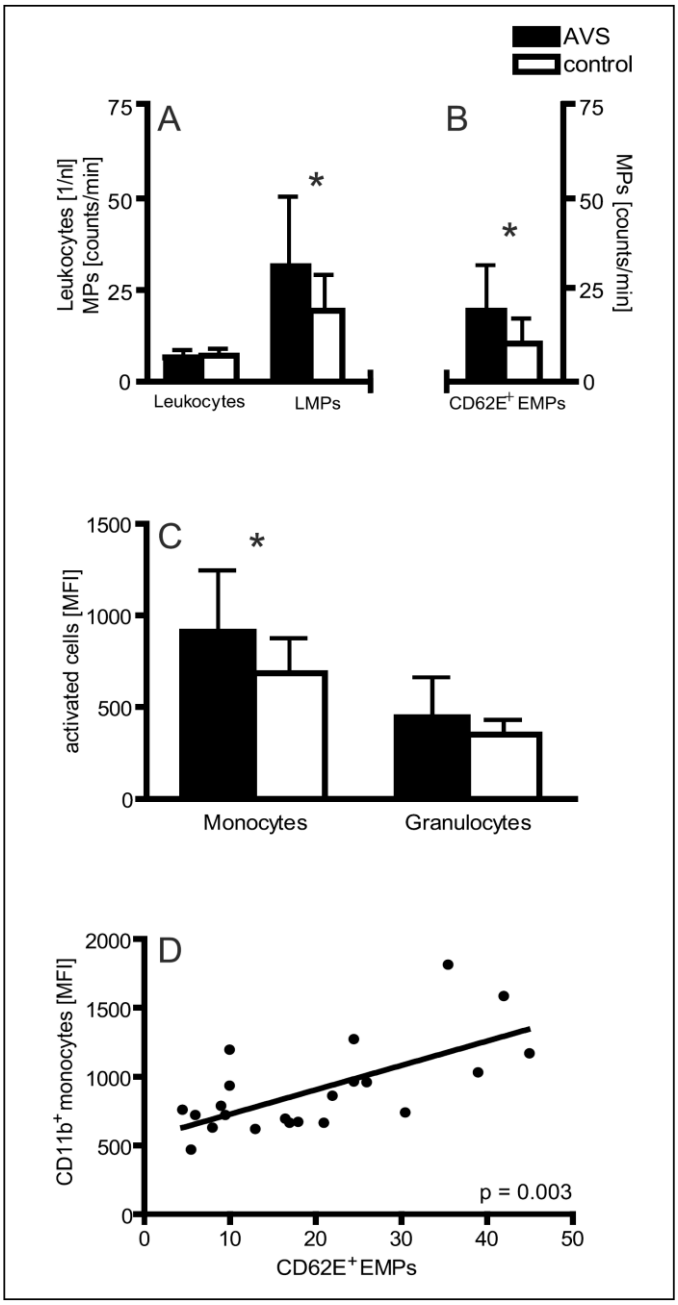

Figure 8. *Leukocyte and endothelial microparticles. A) The total number of leukocytes is similar in AVS patients and patient controls. In contrast, CD11b+ LMPs are increased in AVS patients. B) EMPs resulting from endothelial cell activation (CD62E+) are increased in AVS patients. C) Numbers of activated monocytes are higher in AVS patients compared to patient controls. For activated granulocytes only a trend towards higher numbers in AVS patients could be detected. D) Correlation of CD62E+EMPs and activated monocytes (correlation coefficient 0.66). The parallel generation of activated monocytes and CD62+EMP suggests a pathophysiologic link between these types of particles. * indicates $p<0.05$, AVS versus controls.*

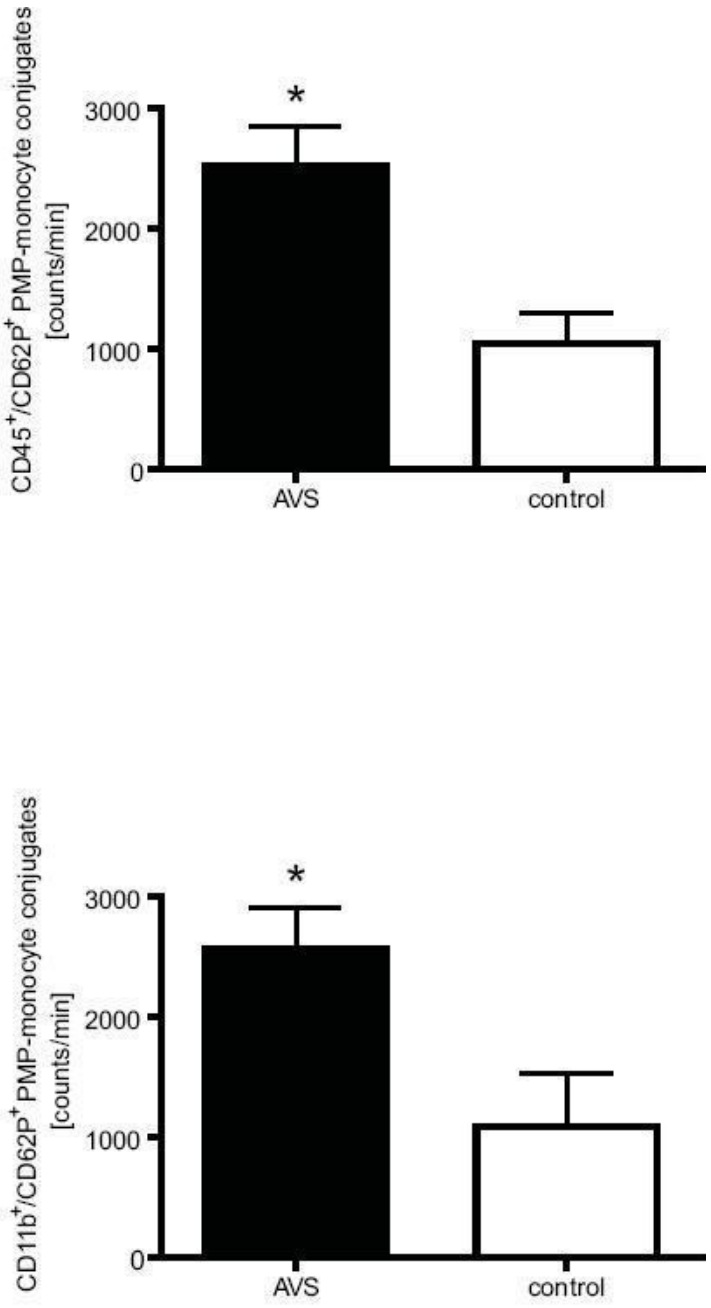

Figure 9. *Formation of PMP-leukocyte conjugates. A) CD45+/CD62P+PMP-monocyte conjugates. AVS patients have more PMP-monocyte conjugates (n =4). B) Most conjugates consist of activated monocytes (CD11b) and PMPs.*

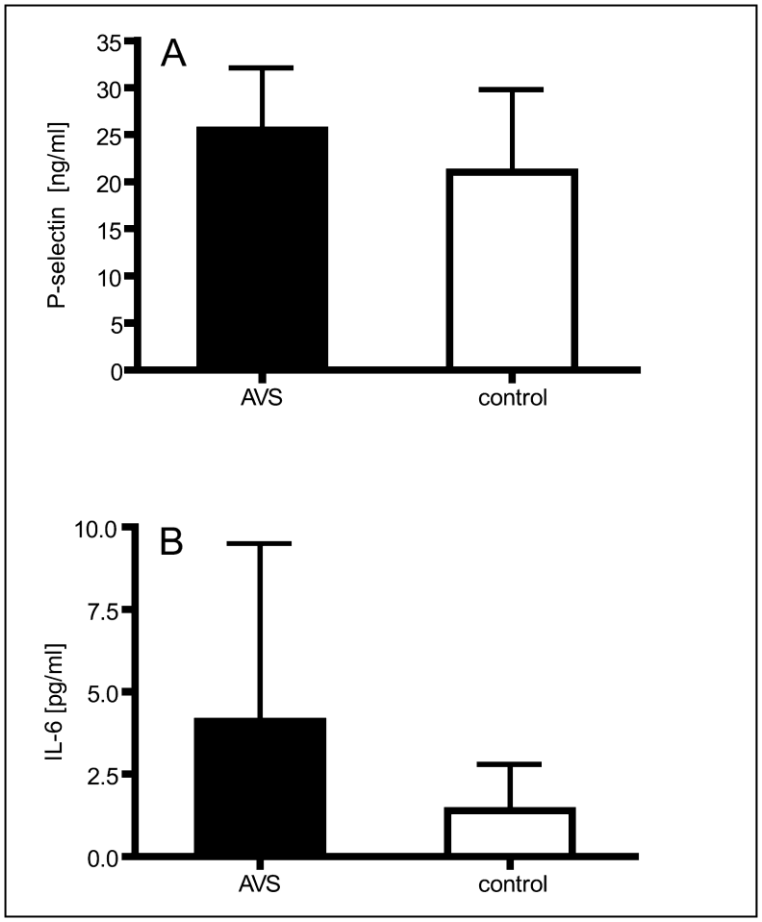

Figure 10. *Plasma markers for platelet activation and systemic inflammation. A) Plasma levels of P-selectin as a marker for platelet activation as determined by ELISA. Levels were not significantly different between groups. B) Interleukin-6 as a marker for systemic inflammation as determined by ELISA. In AVS patients levels tend to be higher although statistical significance is not reached in comparison to patient controls.*

4.2. Evaluation of the relationship between computer-assisted, myocardium selective videodensitometry and TIMI frame count

4.2.1. Clinical parameters

During the present study 124 coronary arteries of 43 patients were analyzed for corrected TFC and G_{max}/T_{max} values. Because of anatomical variations 3 out of 43 left circumflex coronary arteries and 2 out of 43 right coronary arteries were not evaluated. The corrected TFC measured for LAD, CX and RC were comparable to previous data published concerning non-infarct related arteries (55)**.** Clinical and coronary angiographic data on patients are presented in Tables 4-5 respectively.

4.2.2. Correlations

Low to moderate significant correlations were found between corrected TFC of respective arteries and LAD related G_{max}/T_{max} ($r = -0.57$, $p < 0.01$) (Figure 11), CX related G_{max}/T_{max} ($r = -0.33$, $p < 0.05$) (Figure 12) and RC related G_{max}/T_{max} ($r = -0.41$, $p < 0.01$) (Figure 13).

Table 4. Clinical and demographic data of patients.

	Patients
n	43
age (years)	60.2 ± 9.8
Males (%)	29 (67)
Diabetes (%)	5 (12)
Hypertension (%)	35 (79)
Hypercholesterolemia (%)	33 (74)
Smoking (%)	15 (35)

Table 5. Coronary angiography derived data of patients

	Patients
n	43
LAD – G_{max}/T_{max} (1/sec)	2.85 ± 1.56
LAD – cTFC (frames)	25.6 ± 12.1
CX – G_{max}/T_{max} (1/sec)	2.63 ± 1.36
CX – TFC (frames)	25.8 ± 9.7
RC – G_{max}/T_{max} (1/sec)	2.39 ± 0.95
RC – TFC (frames)	26.0 ± 9.9

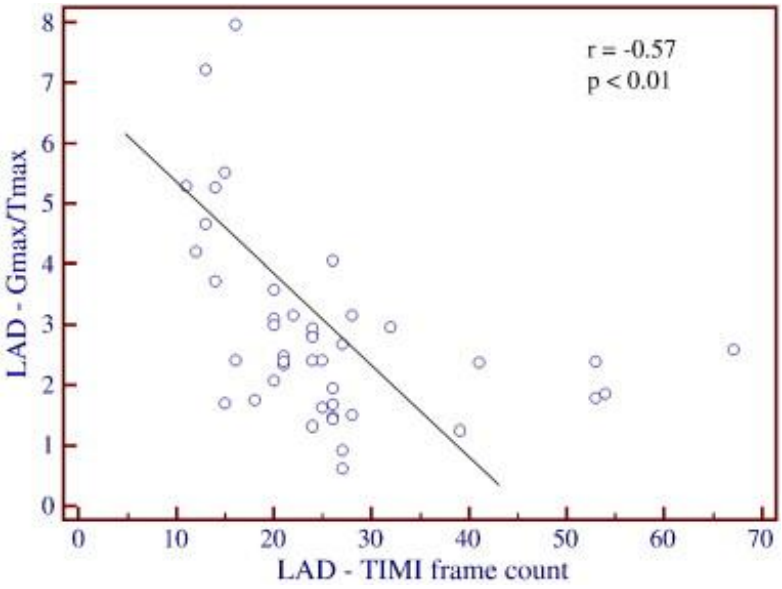

Figure 11. *Correlation between left anterior descending coronary artery (LAD)-related G_{max}/T_{max} and corrected TIMI frame count.*

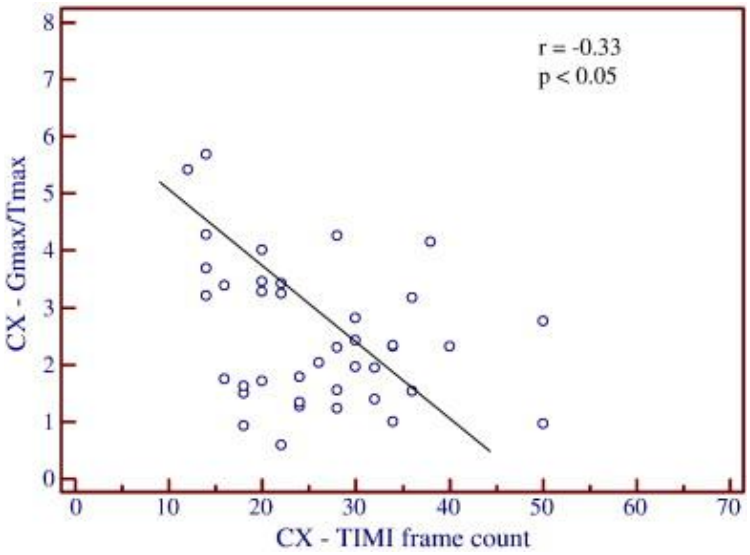

Figure 12. *Correlation between left circumflex coronary artery (CX)-related G_{max}/T_{max} and TIMI frame count.*

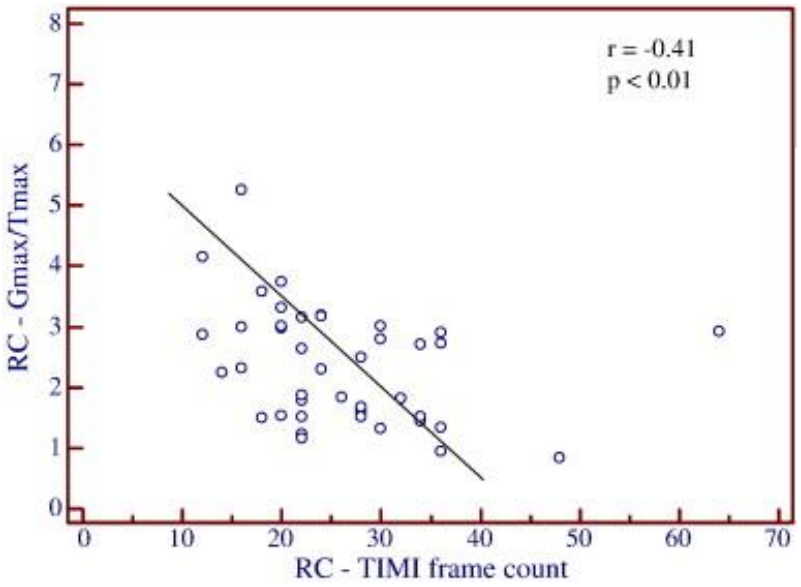

Figure 13. *Correlation between right coronary artery (RC)-related G_{max}/T_{max} and TIMI frame count.*

4.3. Myocardial perfusion abnormalities in aortic valve stenosis as assessed by computer-assisted, myocardium selective videodensitometry

4.3.1. Clinical parameters

In the third study we performed computer assisted, myocardium selective videodensitometric analysis to obtain G_{max}/T_{max} values indicative of myocardial perfusion in 144 coronary arteries of 20 AS and 30 control patients. Because of anatomical variations 3 out of 20 right coronary arteries in the AS group and 2 out of 30 right coronaries as well as 1 out of 30 circumflex arteries in the control group were not evaluated. In regards to clinical and demographic data ASA patients and the control group was similar except for age as the patients in the AS group patients were significantly older (Table 6).

Table 6. Clinical characteristics of aortic valve stenosis patients and patient controls.

	AVS patients	Control patients	p value
N	20	30	-
Male gender (%)	12 (60)	20 (67)	NS
Age (years)	69 ± 10	60 ± 11	<0.05
Diabetes mellitus (%)	5 (25)	4 (13)	NS
Hypercholesterolemia (%)	10 (50)	23 (77)	NS
Hypertension (%)	18 (85)	25 (83)	NS
Smoking (%)	20	13 (43)	NS

4.3.2. Echocardiographic parameters

Peak transvalvular gradient was 84.2 ± 32.5 mmHg and mean transvalvular gradient was 47.4 ± 15.2 mmHg as measured by transthoracic echocardiography reflecting the severity of disease in the AVS group (14). Further echocardiograph parameters of the AS patient group can be found in Table 7.

Table 7. Echocardiographic parameters of aortic valve stenosis patients

	AVS patients (n= 20)
Peak transvalvular aortic gradient (mmHg)	84.2 ± 32.5
Mean transvalvular aortic gradient (mmHg)	47.4 ± 15.2
Left ventricular ejection fraction (%)	59.6 ± 13.7
Left ventricular end-diastolic diameter (mm)	55.9 ± 6.4
Interventricular septum (mm)	13.1 ± 1.6
Left ventricular posterior wall (mm)	12.8 ± 1.5

4.3.3. Computer-assisted, myocardium selective videodensitometry

In the AVS group G_{max}/T_{max} values regarding respective vessels were: LAD-G_{max}/T_{max} =2.78 ± 1.03 1/sec, RC-G_{max}/T_{max} =3.11 ± 1.45 1/sec, CX-G_{max}/T_{max} =2.00 ± 1.13 1/sec). In the control group these values were: LAD-G_{max}/T_{max} =3.44 ± 1.73 1/sec, RC-G_{max}/T_{max} =3.85 ± 1.5 1/sec, CX-G_{max}/T_{max} =2.83 ± 1.04 1/sec. Mean G_{max}/T_{max} describing global myocardial perfusion was 2.55 ± 1.02 1/sec in the AVS group and 3.39 ± 1.09 1/sec in the control group. G_{max}/T_{max} values indicative of myocardial perfusion were significantly lower in the AVS group then in the control group regarding the circumflex artery perfusion territory (p =0.011) and global myocardial perfusion (p =0.008) (Fig. 14). Regarding the left anterior descending artery (p =0.0975) and right coronary artery perfusion territories (p =0.0682) we found a non significant trend towards lower perfusion in the AVS group (Fig 14.).

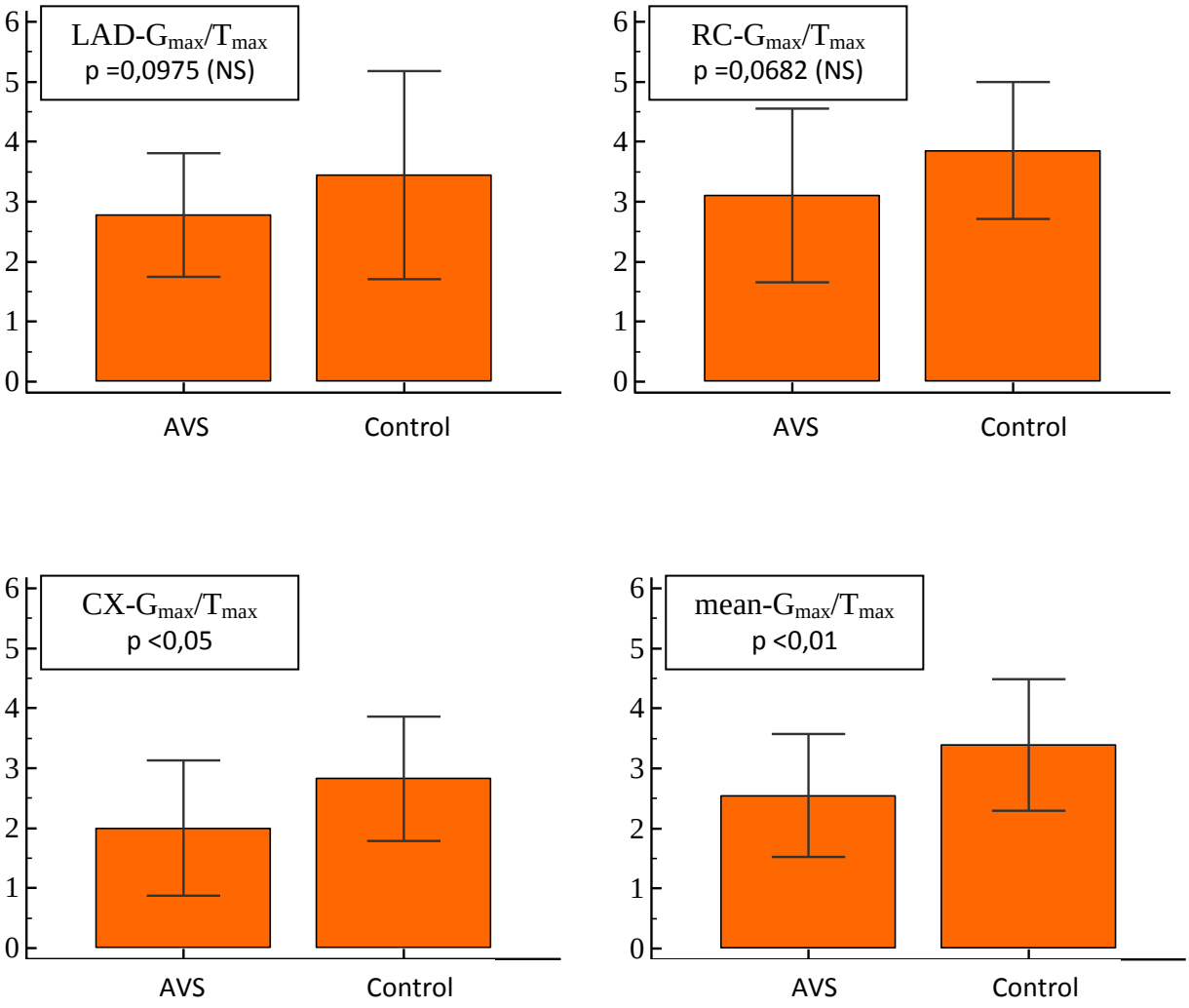

Figure 14. *Mean and respective vessel G_{max}/T_{max} values in the AVS and control group.*

5. DISCUSSION

5.1. Cell derived microparticles in aortic valve stenosis

5.1.1. Elevated shear stress and count of circulating platelet microparticles

The first study presented in this dissertation was performed to determine the level of MP release in patients with severe AVS. We showed for the first time that AVS is accompanied by the release of platelet-, leukocyte-, and endothelial cell-derived MPs and by increased leukocyte activation. PMP release is dependent on shear stress *in vivo* and *in vitro*. We also demonstrated the presence of microparticles conjugated with activated monocytes. These findings indicate that in AVS patients microparticles are released – most probably caused by increased shear stress. Elevated numbers of circulating MPs result in endothelial cell activation (56) which is reflected by EMP release. As the valvular endocardium is a part of the inner lining of the vascular system it is likely but has not been formally demonstrated in this study that valvular endocardium may also be activated by circulating microparticles. Supporting data for this hypothesis comes from studies in which circulating E-selectin, a marker for endothelial cell activation, and E-selectin expression by valvular endocardium is indeed increased in patients with AVS (57). One may speculate whether the activation of valvular endocardium contributes to the progression of AVS, but taking into consideration endothelial cell activation in the context of atherosclerosis this speculation appears justified. We examined patients with severe AVS in comparison to patient controls. Patient controls were admitted for chest pain but cardiovascular disease and particularly valvular disease could be excluded during the hospital stay. In all AVS patients and patient controls confounding conditions such as insulin-dependent diabetes mellitus or infections were excluded (Table 1). Besides the constricted orifice of the aortic valve in AVS patients, both groups were similar in terms of age, concomitant medication and in all other parameters observed (Table 2). As expected, valvular shear stress was significantly higher in AVS patients than in patient controls (Figure 6A). Thus, there is strong evidence that differences observed in microparticle counts and cell activation between the groups are based on differences in blood shear forces. To determine the level of systemic cell activation we measured different types of circulating MPs and activation markers on leukocytes (Figure 1). MPs may serve as markers for cellular activation as they are shed from their particular "cells of origin" upon cell activation. Apart from their role as cell activation markers they confer intercellular communication (15, 58, 59). Increased numbers of circulating MPs have been detected in various conditions such as rheumatic diseases, sepsis, peripheral artery disease and

coagulopathy (16). The common feature of these conditions is their systemic state of inflammation and endothelial cell dysfunction. Here we report that circulating microparticles are increased in AVS patients compared to patient controls. The surface antigens by which PMPs are commonly characterized vary from study to study (51). Most investigators identify PMPs by combined detection of CD31 (PECAM) and CD61 (GPIIIa) surface antigens that are known to be expressed by platelets. In our study, platelet microparticles (CD31+/CD61+), which represent the largest subgroup of all microparticles (AVS: 94.9% vs. PC: 95.0%) and CD62P+PMPs, so called "activated PMPs" are increased in AVS patients (Figure 6B, 6C). Moreover, we found a positive correlation between PMPs and valvular shear stress (Figure 6D). Using an in-vitro flow chamber approach we have confirmed that high shear forces contribute to the formation of PMPs (Figure 7). In our *in vivo* studies we particularly focused on CD62P+PMPs as CD62P is involved in platelet-leukocyte interaction and contributes to vascular diseases such as stroke, myocardial infarction and peripheral artery disease (49, 60, 61). On the molecular level CD62P plays a dual role (62): When measured in plasma samples CD62P reflects the degree of platelet activation. In our study microparticle release was the more sensitive marker of platelet activation compared to CD62P concentrations, which may be explained by the fact that shedding of CD62P from membrane surfaces requires at least in part enzymatic cleavage and therefore occurs later than MP release. On the other hand CD62P is a key mediator in leukocyte interactions in inflammation. We found a trend toward increased CD62P plasma levels in AVS patients that did not reach significance but nonetheless may be in line with this notion. Indeed, in proof-of-principle experiments we found increased numbers of PMP-monocyte conjugates between CD62P+PMPs and monocytes in patients with AVS compared to controls (Figure 9A).

5.1.2. Elevated count of circulating leukocyte, endothelial cell microparticles and systemic inflammation

Taken together, these data suggest that AVS contributes to the generation of PMPs and PMP-monocyte conjugates. Moreover, in depth analysis of PMP-monocyte conjugates revealed that the overwhelming majority of all conjugated monocytes are in the activated state as reflected by expression of CD11b+ (Figure 9B). LMPs are released by monocytes upon cell activation. Therefore, LMPs may be used as a marker for systemic inflammatory reactions. Furthermore, LMPs may act as activators of endothelial cells and thereby actively contribute to systemic inflammation (63) (Fig. 15). Others have shown that the extent of subclinical vascular

dysfunction correlates with the amount of circulating LMPs (64). In the present study we measured LMPs based on the detection of CD11b on microparticles. The integrin CD11b is expressed on activated leukocytes and is involved in adhesion to endothelial cells and transmigration of leukocytes through the endothelial cell layer (50). Using this marker we achieved both, specific detection of leukocyte-derived MPs as well as identification of activated leukocytes. We found that the numbers of CD11b+ LMPs are significantly increased in patients with AVS (Figure 8A). These data suggest that a systemic inflammatory reaction is ongoing in AVS patients. More evidence supporting this notion comes from the detection of elevated numbers of circulating activated monocytes in AVS patients (Figure 8C). Both, LMPs and monocyte activation facilitate transendothelial migration of monocytes initiating vascular inflammation (65). To better characterize a systemic inflammatory state in AVS patients we determined plasma concentrations of IL-6, a well known marker of inflammation, and soluble P-selectin, which is released from activated platelets. In AVS patients IL-6 tends to be higher than in patient controls but the difference does not reach statistical significance (Figure 10B). This finding supports the notion that AVS is associated with systemic inflammation and that MPs may be the more sensitive marker of inflammation compared to IL-6 in these patients. The next step in the cascade of inflammatory events is the activation of endothelial cells. Their activation is reflected by increased levels of circulating EMPs presenting CD62E (E-selectin) as shown in several vascular diseases (66). Using this marker we found that patients with AVS have significantly increased levels of EMPs compared to patient controls (Figure 8B). As vascular endothelium and endocardial cells share a high degree of similarity it is likely that systemic vascular inflammation mediated by MPs and activated leukocytes not only affects vascular endothelium but also the endocardium covering the heart valves and thereby contributes to progression of AVS. Along the same lines, recent studies suggest that inflammatory processes may play a substantial role in the process of cardiac valve thickening and sclerosis, similar to the progression of atherosclerosis (67), although after correction for cardiovascular risk factors inflammatory markers did not predict the extent of valve calcification in one study (68). We suggest that shear stress induces inflammation reflected and conferred by MPs which in turn activate monocytes. Along these lines we found a strong correlation between CD62E+ and activated monocytes (Figure 8D). These cells in turn have been found to incorporate into diseased valves and contribute to disease progression (2). This suggested mechanism is supported by the finding that the incidence of AVS is increased in haemodialysis patients (69). In these patients, high shear stress caused by the haemodialysis procedure may contribute to progression of valve stenosis.

Interestingly, others have shown *in vitro* that endothelial cell-derived MPs contribute to the progression of cardiac valve endocardium dysfunction (70). Accordingly, in rapidly progressing valve disease markers of systemic inflammation such as high-sensitivity CRP are increased (71). These studies put our findings in line with reports that atherosclerosis and AVS depend on similar mechanisms of progression which involve the release of inflammatory MPs (2, 72).

5.1.3. Hypothesis regarding the role of microparticles in the progression of aortic valve stenosis

Taken together based on our in-vivo and in-vitro findings, and supported by *in vitro* findings of other investigators, we suggest a vicious circle in aortic valve disease (Fig. 15): Increased shear forces caused by the constricted aortic valve orifice induce the generation of PMPs in the circulating blood, which in turn interact with circulating monocytes and activate these cells to release LMPs and/or activate vascular endothelial cells directly. Subsequently, LMPs and activated monocytes cause a systemic proinflammatory state, which leads to activation of endothelial cells and release of CD62E+ EMPs. These particles reflect the activation of the endothelium and therefore as well the activation of valvular endocardium. Indeed CD62E serves as an important adhesion molecule involved in leukocyte adhesion on endothelial cells (57). Therefore it may appear possible, but needs to be confirmed by further studies, that activated monocytes transmigrate through the endocardium and contribute to the progression of aortic stenosis. Until today, only monocyte infiltration of diseased cardiac valves has been demonstrated (3, 4).

5.1.4. Limitations

As acknowledged throughout the discussion although data presented here taken together with cited prior observations give strong circumstantial evidence that shear stress generated microparticle interaction with blood cells and endothelium is pivotal in the progression of aortic valve stenosis, they fall short of conclusively establishing a cause-effect relationship. In addition to our cross-sectional study, more definitive support for an active role of microparticles in the pathogenesis of aortic valve stenosis will require a prospective longitudinal study correlating microparticle-cell interaction with progression of aortic valve stenosis.

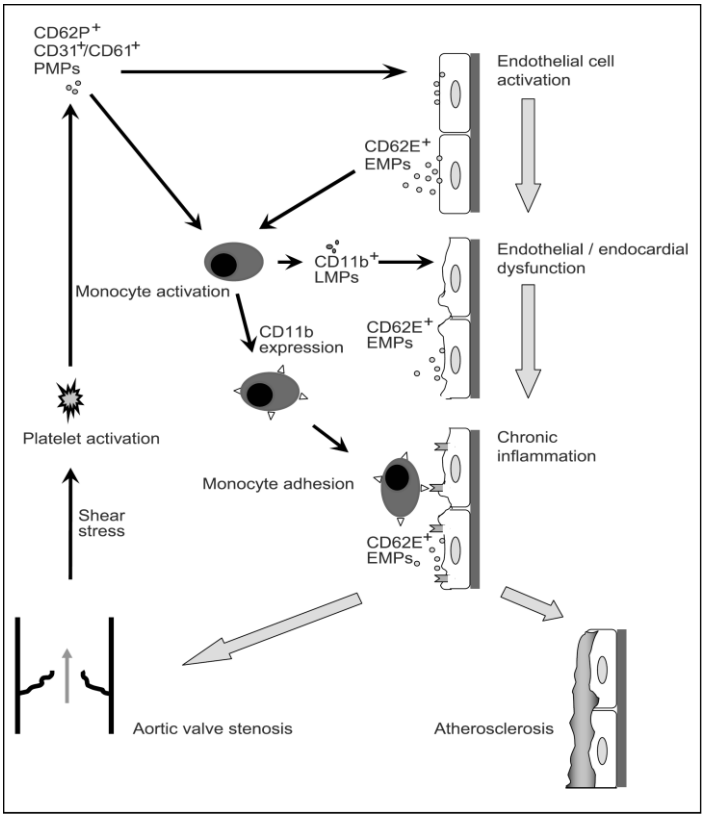

Figure 15. *Suggested model of microparticle pathophysiology and endothelial dysfunction. Platelets are activated by high shear stress and release PMPs. These particles either activate endothelial cells directly or activate mononuclear cells. Mononuclear cell activation is reflected by LMP release and results either directly or via LMPs in endothelial cell activation. In each case endothelial cells are activated as shown by EMP release. Endothelial cell activation contributes to aortic valve stenosis.*

5.2. Myocardial perfusion abnormalities in severe aortic valve stenosis

5.2.1. Evaluation of the relationship of computer-assisted, myocardium selective videodensitometry to TIMI frame count

Myocardium selective videodensitometric assessment of perfusion as MGB and TMPG (described in detail in the introduction section) utilizes the indicator dilution principle where the input is an intracoronary injection of X-ray contrast and the output is observable opacification of the myocardium supplied (73). The degree of opacification representing

perfusion is numerically assessed by the ratio of maximal density (G_{max}) and the time to reach maximum density (T_{max}) of the TDCs in regions of interest on X-ray coronary angiograms (34, 37). This method allows for objective and quantitative assessment, is cost effective without further need for coronary instrumentation. Although well documented in AMI (34-37), literature on possibility of interpretation in non acute coronary syndrome settings is limited (74, 75). Hence before applying computer-assisted, myocardium selective videodensitometry to study possible perfusion abnormalities in aortic valve stenosis we sought to establish its potential use in non-ACS patients by evaluating its relationship to the previous golden standard angiographic method of TFC in patients free of significant coronary artery disease. Correlations could be demonstrated between computerized videodensitometric myocardial blush parameters and quantitative coronary angiographic TFCs (Figures 11-13). Of further note is that stronger correlations were found regarding to LAD compared to RC or CX. Possible explanation for this phenomenon could be coronary anatomy variability, especially concerning the dominance of RC or CX which renders standardized ROI selection. The absence of stronger general correlation in relation to TFC could be explained by the TFC's indirect nature regarding myocardial perfusion, highlighted by its poorer comparable predictive value as previously described in AMI (33). For further validation of this method additional studies are warranted in comparison with established non-angiography-based imaging modalities preferably in specific cardiovascular diseases with microvascular dysfunction.

5.2.2. Myocardial perfusion abnormalities in aortic valve stenosis as assessed by computer-assisted, myocardium selective videodensitometry

The third study presented in this thesis was performed to verify myocardial perfusion abnormalities in severe AVS patients by computer-assisted, myocardium selective densitometry. Previously other authors have described left ventricular mass increment in AVS leading to increased oxygen consumption, decreased arteriole density, coronary diastolic filling impediment and subsequently subendocardial ischemia (8-9). Clinical validation is supplied amongst others by Kupari *et al*. who found perfusion defects in 43% of investigated AVS patients otherwise free of significant epicardial disease by exercise thallium-201 tomography (76). Beside the model dominated by left ventricular pathologic alterations, generalized endothel dysfunction described not only in severe AVS but already in aortic valve sclerosis (10-11) may also play a role in the development of myocardial ischemia, by

affecting the coronary arteries. Elevated count of circulating endothel microparticles reported in the first study of this thesis also supports the notion of generalized endothel dysfunction in AVS. Reduction in coronary flow reserve (CFR) as measured by transoesophageal echocardiography not only directly supplies evidence for coronary microvascular dysfunction (77), but also stresses the relevance of the disorder by proving to be an independent indicator of event-free survival (78). Although myocardial ischemia is certainly most prominent at stress a recent publication by Evola *et al*. describes significant myocardial perfusion impairment at rest by TFC, MBG and scintigraphy in the similar subset of hypertensive patients with left ventricular hypertrophy and angina (79). Based on these previously detailed findings we hypothesized that pathophysiological alterations led by the increment in left ventricular mass and coronary microvascular dysfunction would lead to a slower and less intense penetration of contrast material into the myocardium as quantitatively measured by $G_{max}/T_{max.}$ To test our hypothesis we compared G_{max}/T_{max} values obtained during computer-assisted, myocardium selective videodensitometry in 20 AVS patients to 30 control patients. Groups were similar in regards to gender and cardiac risk factors. The AVS group however was significantly older as discussed in the limitations section. Significant epicardial stenosis was ruled out during coronary angiography in both groups. Indeed mean Gmax/Tmax values indicative of global myocardial perfusion were significantly lower in the AVS group than in the control group (Fig. 14). The observed large standard deviation and only non-significant tendencies in regards to LAD- and RCA-related G_{max}/T_{max} must draw our attention to the limitations of perfusion assessment at rest in non-ACS patients. Namely coronary blood flow, myocardial perfusion and microvascular resistance at rest is mainly determined by hemodynamic parameter driven autoregulation mechanisms (80), and subject to variations according to gender and age (81). In future studies it would seem prudent to uncouple autoregulation of myocardial circulation through achievement of maximal hyperemia by intracoronary or intravenous adenosin infusion (82). G_{max}/T_{max} values at hyperemia by themselves or as a ratio of baseline G_{max}/T_{max} akin to CFR may prove to more specific and sensitive marker of microvascular dysfunction. In conclusion reduced Gmax/Tmax values indicative of impaired myocardial perfusion as measured by computer-assisted myocardium selective videodensitometry on coronary angiograms could be demonstrated in AS compared to normal controls.

5.2.3. Limitations

Computer-assisted, myocardium selective videodensitometry is a novel method under constant development as technological advances permit. Major technical issues yet to be tackled include problems concerning the standardized selection of static ROI areas. Large ROI areas can result in variable results due to inhomogenous distribution of contrast material. On the other hand, small static ROI area selection is difficult for the whole image sequence because of the cyclic motion of myocardium caused by the heart beating. Further problems inherent to nonautomated ROI selection is the possibility of intra- and interobserver variability. These factors in part may be accountable for variable average G_{max}/T_{max} values reported for similar control groups discussed in this thesis and in a prior publication. Of further note is the commercial unavailability of our software and those of others which renders wide spread use and unbiased, multicenter testing.

Mean G_{max}/T_{max} characterizing global myocardium perfusion is calculated as a numerical average of single-vessel-related G_{max}/T_{max} values. It is not weighted to take into count differing vessel sizes and supplied myocardium areas which change from to patient to patient according to anatomical variations.

Echocardiographic studies for the patients were done in different hospitals as part of our preoperative examination protocol and thus are not standardized for the echocardiographic machine used or the examiner itself. Furthermore the most revealing parameter in regards to AVS severity, aortic valve surface area was not measured in all of the patients.

Although efforts were made to match the control group to the AVS group in terms of cardiovascular risk factors, age and gender, the AVS group patients were found to be significantly older. Explanation for this age difference lies in the pathophysiology of AVS as it is an age-related, degenerative disease prominent and necessitating surgery most frequently in patients older than 65 years. Nonetheless this factor must be taken into account while interpreting our results.

SUMMARY

The mechanisms of the progression of AVS are partly unknown. The involvement of mononuclear cells and of chronic systemic inflammation has been suggested by analysis of pathological specimens. In the first study reported in this thesis we hypothesized that shear stress caused by the constricted aortic orifice contributes to systemic proinflammation by activation of circulating blood cells and thereby generation of microparticles. Using flow cytometry we analyzed 22 patients with severe AVS and 18 patient controls for the generation of circulating microparticles from platelet- (PMPs: CD31+/CD61+ or CD62P+), leukocyte- (LMPs: CD11b+) and endothelial cell (EMPs: CD62E+) origin. Apart from the constricted valve orifice groups were similar. PMPs were increased in AVS patients and their number correlated with valvular shear stress. Monocytes were activated in AVS patients, an observation that was also reflected by increased numbers of LMPs and by the detection of PMP-monocyte conjugates. Furthermore, EMPs reflecting the activation of endothelial cells but also conferring systemic inflammatory activity were increased in AVS patients and correlated with the number of activated monocytes. In conclusion, we showed that AVS is accompanied by increased levels of microparticles and that shear stress can induce the formation of microparticles. Based on our results and histological findings of other investigators the speculation that shear stress related to AVS induces a vicious circle including the generation of PMPs, the subsequent activation of monocytes and LMPs and finally the activation of endothelial cells contributing to the progress of AVS appears to be justified.

Recently alongside others we have introduced a novel computer-assisted videodensitometric method for the quantitative assessment of the angiographic “blush” appearance in AMI. We have characterized myocardial perfusion by the ratio of maximal density and the time to reach maximum density of the time–density curves in regions of interest on X-ray coronary angiograms. Although well documented in AMI, literature on possibility of interpretation in non-acute coronary syndrome settings is limited. In the second study comprising this thesis we set out to establish the potential use of this method in non-ACS patients (for example in AVS) by evaluating its relationship to the previous golden standard angiographic method of TFC in patients free of significant coronary artery disease. Significant correlations could be demonstrated between computerized videodensitometric myocardial blush parameters and quantitative coronary angiographic TFCs. For further validation of this method additional

studies are warranted in comparison with established non-angiography-based imaging modalities.

The third study presented in thesis was performed to further verify myocardial perfusion abnormalities present in severe AVS patients. For this purpose we measured G_{max}/T_{max} values indicative of myocardial perfusion by computer-assisted, myocardium selective videodensitometry in 20 AVS patients and 30 control patients. Significant epicardial stenosis was ruled out during coronary angiography in both groups. We hypothesized that pathophysilogical alterations led by an increment in left ventricular mass and generalized microvascular dysfunction would lead to a slower and less intense penetration of contrast material as quantitatively measured by $G_{max}/T_{max.}$ Indeed mean G_{max}/T_{max} values indicative of global myocardial perfusion were significantly lower in the AVS group then in the control group. In conclusion reduced G_{max}/T_{max} values indicative of impaired myocardial perfusion as measured by densitometry on coronary angiograms could be demonstrated in AS compared to normal controls.

CONCLUSIONS (NEW OBSERVATIONS)

- Severe AVS is accompanied by increased levels of circulating microparticles and monocyte activation.
- Shear stress induces the formation of microparticles both *in vitro* and in AVS *in vivo.*
- Based on our results and histological findings of other investigators a novel hypothesis may be formed that shear stress related to AVS induces a vicious circle including the generation of platelet microparticles, the subsequent activation of monocytes and leukocyte microparticles and finally the activation of endothelial cells contributing to the progress of aortic valve stenosis
- Significant correlations exist between computer-assisted, myocardium selective videodensitometry-derived parameters and quantitative coronary angiographic TFCs in patients free of significant epicardial disease indicating possible usefulness of this method in the non-acute coronary syndrome patient population.
- Reduced Gmax/Tmax values indicative of impaired myocardial perfusion can be demonstrated by computer-assisted, myocardium selective videodensitometry on coronary angiograms in severe AVS compared to normal controls.

REFERENCES

1. Stewart BF, Siscovick D, Lind BK et al. Clinical factors associated with calcific aortic valve disease. Cardiovascular Health Study. J Am Coll Cardiol 1997; 29:630–4
2. Iung B, Baron G, Butchart EG et al. A prospective survey of patients with valvular heart disease in Europe: the Euro Heart Survey on valvular heart disease. Eur Heart J 2003; 24:1231–43.
3. Galante A, Pietroiusti A, Vellini M et al. C-reactive protein is increased in patients with degenerative aortic valvular stenosis. J Am Coll Cardiol 2001; 38: 1078–1082
4. O'Brien KD. Pathogenesis of calcific aortic valve disease: a disease process comes of age (and a good deal more). Arterioscler Thromb Vasc Biol 2006; 8:1721-8.
5. Mazzone A, Epistolato MC, Gianetti J et al. Biological features (inflammation and neoangiogenesis) and atherosclerotic risk factors in carotid plaques and calcified aortic valve stenosis: two different sites of the same disease? Am J Clin Pathol 2006; 126: 494–502.
6. Otto CM. Calcific aortic stenosis--time to look more closely at the valve. N Engl J Med 2008; 359:1395-8.
7. Bonow OR, Mann LD, Zipes PD et al. Braunwald's heart disease. A textbook of cardiovascular medicine 2011; 1468-1478
8. Nadell R, DePace NL, Ren JF et al. Myocardial oxygen supply/demand in aortic stenosis: hemodynamic and echocardiographic evaluation of patients with and without angina pectoris. J Am Coll Cardiol 1983; 2: 258–262
9. Marcus ML, Koyanagi S, Harrison DG et al. Abnormalities in the coronary circulation that occur as a consequence of cardiac hypertrophy. Am. J. Med 1983; 75: 62–66
10. Poggianti E, Venneri L, Chubuchny V et al. Aortic valve sclerosis is associated with systemic endothelial dysfunction. J. Am. Coll. Cardiol 2003; 41: 136–141.
11. Yamaura Y, Nishida T, Watanabe et al. Relation of aortic valve sclerosis to carotid artery intima-media thickening in healthy subjects. Am J Cardiol 2004; 94: 837-839.
12. Chan KL, Teo K, Dumesnil JG et al. Effect of Lipid lowering with rosuvastatin on progression of aortic stenosis: results of the aortic stenosis progression observation: measuring effects of rosuvastatin (ASTRONOMER) trial. Circulation. 2010; 121: 306-14.

13. Rossebø AB, Pedersen TR, Boman K et al. Intensive lipid lowering with simvastatin and ezetimibe in aortic stenosis. N Engl J Med 2008; 359: 1343-56.

14. Bonow RO, Carabello BA, Kanu C et al. ACC/AHA 2006 guidelines for the management of patients with valvular heart disease: a report of the American College of Cardiology/American Heart Association Task Force on Practice Guidelines (writing committee to revise the 1998 Guidelines for the Management of Patients With Valvular Heart Disease): developed in collaboration with the Society of Cardiovascular Anesthesiologists: endorsed by the Society for Cardiovascular Angiography and Interventions and the Society of Thoracic Surgeons. American College of Cardiology/American Heart Association Task Force on Practice Guidelines; Society of Cardiovascular Anesthesiologists; Society for Cardiovascular Angiography and Interventions; Society of Thoracic Surgeons. Circulation 2006; 114:84-231.

15. Martinez MC, Tesse A, Zobairi F et al. Shed membrane microparticles from circulating and vascular cells in regulating vascular function. Am J Physiol Heart Circ Physiol 2005; 288: H1004–1009.

16. Hugel B, Martinez MC, Kunzelmann C et al. Membrane microparticles: two sides of the coin. Physiology (Bethesda) 2005; 20: 22–27.

17. Sabatier F, Roux V, Anfosso F et al. Interaction of endothelial microparticles with monocytic cells in vitro induces tissue factor-dependent procoagulant activity. Blood 2002; 99: 3962–3970.

18. Distler JH, Pisetsky DS, Huber LC et al. Microparticles as regulators of inflammation: novel players of cellular crosstalk in the rheumatic diseases. Arthritis Rheum 2005; 52: 3337–3348.

19. Koga H, Sugiyama S, Kugiyama K et al. Elevated levels of remnant lipoproteins are associated with plasma platelet microparticles in patients with type-2 diabetes mellitus without obstructive coronary artery disease. Eur Heart J 2006; 27: 817–823.

20. Barry OP, Pratico D, Lawson JA et al. Transcellular activation of platelets and endothelial cells by bioactive lipids in platelet microparticles. J Clin Invest 1997; 99: 2118–2127.

21. Daniel L, Fakhouri F, Joly D et al. Increase of circulating neutrophil and platelet microparticles during acute vasculitis and hemodialysis. Kidney Int 2006; 69: 1416–1423.

22. Esposito K, Ciotola M, Schisano B et al. Endothelial microparticles correlate with endothelial dysfunction in obese women. J Clin Endocrinol Metab 2006; 91: 3676–3679.

23. Mezentsev A, Merks RM, O'Riordan E et al. Endothelial microparticles affect angiogenesis in vitro: role of oxidative stress. Am J Physiol Heart Circ Physiol 2005; 289: H1106–1114.

24. Gibson CM, Cannon CP, Daley WL et al. TIMI frame count: a quantitative method of assessing coronary artery flow. Circulation. 1996; 93: 879-88

25. Kunadian V, Harrigan C, Zorkun C et al. Use of the TIMI frame count in the assessment of coronary artery blood flow and microvascular function over the past 15 years. J Thromb Thrombolysis 2009; 27: 316-28.

26. Turhan H, Erbay AR, Yasar AS et al. Impaired coronary blood flow in patients with metabolic syndrome: documented by Thrombolysis in Myocardial Infarction (TIMI) frame count method. Am Heart J 2004; 148: 789-94.

27. Barutcu I, Turkmen M, Sezgin AT et al. Increased thrombolysis in myocardial infarction (TIMI) frame count in patients with aortic stenosis but normal coronary arteries. Heart Vessels. 2005; 3: 108-11.

28. Yasar AS, Turhan H, Erbay AR et al. Assessment of coronary blood flow in hypertrophic cardiomyopathy using thrombolysis in myocardial infarction frame count method. J Invasive Cardiol 2005; 17: 73-6.

29. Baris N, Sipahi I, Kapadia SR et al. Coronary angiography for follow-up of heart transplant recipients: insights from TIMI frame count and TIMI myocardial perfusion grade. J Heart Lung Transplant 2007; 26: 593–597

30. Luo C, Wu X, Huang Z et al. Documentation of impaired coronary blood flow by TIMI frame count method in patients with atrial fibrillation. Int J Cardiol 2012; [Epub ahead of print]

31. Porto I, Hamilton-Craig C, Brancati M et al. Angiographic assessment of microvascular perfusion--myocardial blush in clinical practice. Am Heart J 2010; 160: 1015-22.

32. van't Hof AW, Liem A, Suryapranata H et al. Angiographic assessment of myocardial reperfusion in patients treated with primary angioplasty for acute myocardial infarction: myocardial blush grade. Zwolle Myocardial Infarction Study Group. Circulation 1998; 97: 2302-6.

33. Gibson CM, Cannon CP, Murphy SA et al. Relationship of TIMI myocardial perfusion grade to mortality after administration of thrombolytic drugs. Circulation 2000; 101: 125-30

34. Korosoglou G, Haars A, Michael G et al. Quantitative evaluation of myocardial blush to assess tissue level reperfusion in patients with acute ST-elevation myocardial infarction: incremental prognostic value compared with visual assessment. Am Heart J 2007; 153: 612-20.

35. Haeck JD, Gu YL, Vogelzang M et al. Feasibility and applicability of computer-assisted myocardial blush quantification after primary percutaneous coronary intervention for ST-segment elevation myocardial infarction. Catheter Cardiovasc Interv 2010; 75: 701-706.

36. Vogelzang M, Vlaar PJ, Svilaas T et al: Computer-assisted myocardial blush quantification after percutaneous coronary angioplasty for acute myocardial infarction: a substudy from the TAPAS trial. Eur Heart J 2009; 30: 594-599.

37. Ungi T, Ungi I, Jónás Z et al. Myocardium selective densitometric perfusion assessment after acute myocardial infarction. Cardiovasc Revasc Med 2009; 10: 49-54.

38. Ungi T, Zimmermann Z, Balázs E et al. Vessel masking improves densitometric myocardial perfusion assessment. Int J Cardiovasc Imaging 2009; 25: 229-36

39. Boulanger CM, Scoazec A, Ebrahimian T et al. Circulating microparticles from patients with myocardial infarction cause endothelial dysfunction. Circulation 2001; 104: 2649–2652.

40. Arteaga RB, Chirinos JA, Soriano AO et al. Endothelial microparticles and platelet and leukocyte activation in patients with the metabolic syndrome. Am J Cardiol 2006; 98: 70–74.

41. Beckman JA, Creager MA, Libby P. Diabetes and atherosclerosis: epidemiology, pathophysiology, and management. J Am Med Assoc 2002; 287: 2570–2581.

42. van der Zee PM, Biro E, Ko Y et al. P-selectin- and CD63-exposing platelet microparticles reflect platelet activation in peripheral arterial disease and myocardial infarction. Clin Chem 2006; 52: 657–664.

43. Morel N, Morel O, Delabranche X et al. Microparticles during sepsis and trauma. A link between inflammation and thrombotic processes. Ann Fr Anesth Reanim 2006; 25: 955–966.

44. Ogura H, Tanaka H, Koh T et al. Enhanced production of endothelial microparticles with increased binding to leukocytes in patients with severe systemic inflammatory response syndrome. J Trauma 2004; 56: 823–830; discussion 830–821.

45. Minagar A, Jy W, Jimenez JJ et al. Elevated plasma endothelial microparticles in multiple sclerosis. Neurology 2001; 56: 1319–1324.

46. Amabile N, Guerin AP, Leroyer A et al. Circulating endothelial microparticles are associated with vascular dysfunction in patients with end-stage renal failure. J Am Soc Nephrol 2005; 16: 3381–3388.

47. Kim HK, Song KS, Park YS et al. Elevated levels of circulating platelet microparticles, VEGF, IL-6 and RANTES in patients with gastric cancer: possible role of a metastasis predictor. Eur J Cancer 2003; 39: 184–191.

48. Lang RM, Bierig M, Devereux RB et al. Recommendations for chamber quantification: a report from the American Society of Echocardiography's Guidelines and Standards Committee and the Chamber Quantification Writing Group, developed in conjunction with the European Association of Echocardiography, a branch of the European Society of Cardiology. J Am Soc Echocardiogr 2005; 18: 1440–1463.

49. Keuren JF, Magdeleyns EJ, Govers-Riemslag JW et al. Effects of storage-induced platelet microparticles on the initiation and propagation phase of blood coagulation. Br J Haematol 2006; 134: 307–313.

50. Fujimi S, Ogura H, Tanaka H et al. Increased production of leukocyte microparticles with enhanced expression of adhesion molecules from activated polymorphonuclear leukocytes in severely injured patients. J Trauma 2003; 54: 114–120.

51. Jy W, Horstman LL, Jimenez JJ, et al. Measuring circulating cell-derived microparticles. J Thromb Haemost 2004; 2: 1842–1843.

52. Jy W, Mao WW, Horstman L et al. Platelet microparticles bind, activate and aggregate neutrophils in vitro. Blood Cells Mol Dis 1995; 21: 217–231.

53. Chirinos JA, Heresi GA, Velasquez H et al. Elevation of endothelial microparticles, platelets, and leukocyte activation in patients with venous thromboembolism.J Am Coll Cardiol 2005; 45: 1467–1471.

54. Ahrens IG, Moran N, Aylward K et al. Evidence for a differential functional regulation of the two beta(3)-integrins alpha(V)beta(3) and alpha(IIb)beta(3). Exp Cell Res 2006; 312: 925–937.

55. Vijayalakshmi K, Ashton VJ, Wright RA et al. Corrected TIMI frame count: applicability in modern digital catheter laboratories when different frame acquisition rates are used Catheter Cardiovasc Interv. 2004; 63: 426-32.

56. Mesri M, Altieri DC. Endothelial cell activation by leukocyte microparticles. J Immunol 1998; 161: 4382–4387.

57. Ghaisas NK, Foley JB, O'Briain DS et al. Adhesion molecules in nonrheumatic aortic valve disease: endothelial expression, serum levels and effects of valve replacement. J Am Coll Cardiol 2000; 36: 2257–2262.

58. Pfister SL. Role of platelet microparticles in the production of thromboxane by rabbit pulmonary artery. Hypertension 2004; 43: 428–433.

59. Joop K, Berckmans RJ, Nieuwland R et al. Microparticles from patients with multiple organ dysfunction syndrome and sepsis support coagulation through multiple mechanisms. Thromb Haemost 2001; 85: 810–820.

60. Cauwenberghs S, Feijge MA, Harper AG et al. Shedding of procoagulant microparticles from unstimulated platelets by integrin-mediated destabilization of actin cytoskeleton. FEBS Lett 2006; 580: 5313–5320.

61. Atkinson C, Zhu H, Qiao F et al. Complement-dependent P-selectin expression and injury following ischemic stroke. J Immunol 2006; 177: 7266–7274.

62. Polgar J, Matuskova J, Wagner DD. The P-selectin, tissue factor, coagulation triad. J Thromb Haemost 2005; 3: 1590–1596.

63. Mesri M, Altieri DC. Leukocyte microparticles stimulate endothelial cell cytokine release and tissue factor induction in a JNK1 signaling pathway. J Biol Chem 1999; 274: 23111–23118.

64. Chironi G, Simon A, Hugel B et al. Circulating leukocyte-derived microparticles predict subclinical atherosclerosis burden in asymptomatic subjects. Arterioscler Thromb Vasc Biol 2006; 26: 2775–2780.

65. Jy W, Minagar A, Jimenez JJ et al. Endothelial microparticles (EMP) bind and activate monocytes: elevated EMP-monocyte conjugates in multiple sclerosis. Front Biosci 2004; 9: 3137–3144.

66. Brogan PA, Dillon MJ. Endothelial microparticles and the diagnosis of the vasculitides. Intern Med 2004; 43: 1115–1119.

67. Poggianti E, Venneri L, Chubuchny V et al. Aortic valve sclerosis is associated with systemic endothelial dysfunction. J Am Coll Cardiol 2003; 41: 136–141.

68. Fox CS, Guo CY, Larson MG et al. Relations of inflammation and novel risk factors to valvular calcification. Am J Cardiol 2006; 97: 1502–1505.

69. Schonenberger A, Winkelspecht B, Kohler H et al. High prevalence of aortic valve alterations in haemodialysis patients is associated with signs of chronic inflammation. Nephron Clin Pract 2004; 96: c48–55.

70. Klinkner DB, Densmore JC, Kaul S et al. Endothelium-derived microparticles inhibit human cardiac valve endothelial cell function. Shock 2006; 25: 575–580.

71. Sanchez PL, Santos JL, Kaski JC et al. Relation of circulating C-reactive protein to progression of aortic valve stenosis. Am J Cardiol 2006; 97: 90–93.

72. Sanchez PL, Mazzone A. C-reactive protein in degenerative aortic valve stenosis. Cardiovasc Ultrasound 2006; 4: 24.

73. Leung DY, Leung M. Non-invasive/invasive imaging: significance and assessment of coronary microvascular dysfunction. Heart 2011; 97: 587-95.

74. Havers J, Haude M, Erbel R et al. X-ray densitometric measurement of myocardial perfusion reserve in symptomatic patients without angiographically detectable coronary stenoses. Herz 2008;, 33: 223-232.

75. Korosoglou G, Riedle N, Erbacher M et al. Quantitative myocardial blush grade for the detection of cardiac allograft vasculopathy. Am Heart J 2010; 159: 643-651.

76. Kupari M, Virtanen KS, Turto H et al. Exclusion of coronary artery disease by exercise thallium-201 tomography in patients with aortic valve stenosis. Am J Cardiol 1992; 70: 635–640

77. Nemes A, Forster T, Varga A et al. How can coronary flow reserve be altered by severe aortic stenosis? Echocardiography 2002; 19: 655–669.

78. Nemes A, Balazs E, Csanady M et al. Long-term prognostic role of coronary flow velocity reserve in patients with aortic valve stenosis - insights from the SZEGED Study. Clin Physiol Funct Imaging 2009; 29: 447-52.

79. Evola S, Cuttitta F, Evola G et al. Early Detection of Coronary Artery Flow and Myocardial Perfusion Impairment in Hypertensive Patients Evidenced by Myocardial Blush Grade (MBG) and Thrombolysis in Myocardial Infarction (TIMI) Frame Count (TFC). Intern Med 2012; 51: 1653-60.

80. Braunwald E. Control of myocardial oxygen consumption: physiologic and clinical considerations. Am J Cardiol 1971; 27: 416–432

81. Kaufmann, P.A., Camici, P.G.: Myocardial blood flow by PET: technical aspects and clinical applications. J Nucl Med; 2005: 46, 75-88.

82. Kern MJ, Lerman A, Bech JW et al. Physiological assessment of coronary artery disease in the cardiac catheterization laboratory: a scientific statement from the American Heart Association Committee on Diagnostic and Interventional Cardiac Catheterization, Council on Clinical Cardiology. Circulation 2006; 114: 1321–1341

ACKNOWLEDGEMENT

First of all I would like to thank my wife Zsuzsa and my sons Balázs and Zalán for their support and patience during the long and tiresome road needed to complete this thesis.

I would also like to thank my mother, father and uncle not only for their support but also for serving as excellent role models with their pre-eminent academic careers.

I am most grateful to Professor Martin Moser for providing me with an excellent and stimulating atmosphere for doing research at the University of Freiburg and for willing me on in the troubled beginning period when I thought microparticle isolation is not possible.

I would like to express my deepest gratitude to Dr. Imre Ungi who is not only my mentor in the field of interventional cardiology but together with his son Dr. Tamás Ungi the founder of the computer-assisted myocardium selective videodensitometric method for assessment of myocardial perfusion discussed in the second part of this thesis.

I would never have been able to finish my dissertation without the guidance of my supervisors Dr. Attila Nemes and Professor Tamás Forster who never let me lose sight of my final goal.

Last but not least I would like to thank my colleagues here at the University of Szeged who not only helped in recruiting patients for my study but also substituted me in every day clinical practice during my year abroad.